

ALTERED PURKINJE CELL PACEMAKING UNDERLIES MOTOR DEFICITS IN
MOUSE MODELS OF CEREBELLAR ATAXIA

by

Forrest Davis

A DISSERTATION

Presented to the Vollum Institute
and the Oregon Health & Science University
School of Medicine
in partial fulfillment of
the requirements for the degree of
Doctor of Philosophy
June 2010

School of Medicine
Oregon Health & Science University

CERTIFICATE OF APPROVAL

This is to certify that the Ph.D. dissertation of
FORREST X DAVIS
has been approved

Advisor, John Adelman, Ph.D.

Advisor, James Maylie, Ph.D.

Member and Chair, Gary Westbrook, M.D.

Member, Matthew Frerking, Ph.D.

Table of Contents

Acknowledgments.....	ii
Abstract.....	iii
I. Introduction.....	1
Potassium channels	1
The cerebellum.....	7
Episodic Ataxia type 1.....	17
SK2.....	30
II. The Cellular Basis of Episodic Ataxia Type1	39
III. Reduced expression of SK2 alters intrinsic Purkinje cell firing and motor coordination.....	75
IV. Discussion.....	112
V. Summary and Conclusions.....	123
VI. Bibliography.....	125

*With gratitude to my mentors Jim Maylie and John Adelman,
and to my family.*

Abstract

Purkinje cells play a central role in motor coordination and movement, two processes that are compromised by cerebellar ataxias. Purkinje cells are called pacemakers because they exhibit an intrinsically generated, tonic firing pattern. The intrinsic firing pattern of Purkinje cells is modified by inhibitory and excitatory input, and constitutes the sole output from the cerebellar cortex. Therefore, aberrations in cerebellar processing are encoded as a modified Purkinje cell output. For example, a decrease in the precision of Purkinje cell pacemaking has been implicated in ataxia. Episodic ataxia/myokymia type 1 (EA1) is caused by mutations of the voltage-gated potassium channel Kv1.1. In patients with EA1, physical or emotional stress can trigger attacks of imbalance and loss of motor control. The carbonic anhydrase inhibitor acetazolamide reduces the frequency and severity of these attacks.

In this thesis, I first examined a mouse model of EA1, and sought to determine whether imprecision of Purkinje cell pacemaking causes the stress-induced motor deficits. Increased GABAergic inhibition in Purkinje cells reduced the precision of Purkinje cell pacemaking. The precision deficit was exacerbated by β -adrenergic receptor activation, a model of the effects of stressful events that can precipitate attacks in patients with EA1. The precision deficit was ameliorated by acetazolamide, which also occluded the effects of subsequent β -adrenergic receptor activation. These results suggest that alteration of Purkinje cell pacemaking underlies ataxia in EA1.

In the second half of this thesis, I analyzed the relationship between Purkinje cell pacemaking precision and motor coordination in a mouse with reduced expression of the small conductance Ca^{2+} activated potassium channel SK2 ($\text{SK2}^{\text{fl/fl}}$). Ca^{2+} -activated potassium currents are central to the timing of action potentials. Purkinje cells in $\text{SK2}^{\text{fl/fl}}$ mice displayed irregular pacemaking in the majority of lobules (I-VII) within the cerebellar vermis, but this deficit did not affect motor skills as measured by balance beam and accelerating rotarod assays. A minority of the cerebellar cortex, comprised of lobules VIII and IX, had normal Purkinje cell pacemaking in $\text{SK2}^{\text{fl/fl}}$ animals. Ablation of this region removed all regular Purkinje cell firing from the $\text{SK2}^{\text{fl/fl}}$ vermis, and unmasked a motor deficit assayed by the balance beam. This result supports the notion that Purkinje cell pacemaking is required for cerebellar-dependent motor tasks. Conversely, lobule VIII/IX ablation failed to elicit a performance deficit on the accelerating rotarod in $\text{SK2}^{\text{fl/fl}}$ mice, suggesting that regular Purkinje cell firing in the vermis is not required for all cerebellar-dependent tasks.

I. INTRODUCTION

The K⁺ channel superfamily

The distinguishing feature of all potassium channels is selective potassium conductance. Potassium-selective channels comprise the largest and most diverse superfamily of ion channels, with over 70 known mammalian genes (Yu et al., 2005). With this variety of genes, it is not surprising that potassium channels play a role in most, if not all, living cells. Indeed, most cell types express many different potassium channel family members (Miller, 2000). Potassium channels are activated by various stimuli, including depolarization, hyperpolarization, Ca²⁺, and ATP. In non-neuronal cells, potassium channels perform a range of functions that include control of heart rate and hormone secretion. In the cells of the nervous system, potassium channels are central to controlling membrane excitability. Because the reversal potential for potassium is negative to resting potential in neurons, opening of these channels tends to dampen excitability. The exception is inwardly rectifying potassium channels, briefly described below. Electrical dampening by potassium channel activity has varied effects depending on the neuronal subtype and the cellular compartment. These include control of membrane resting potential, counter-balancing membrane depolarization by synaptic inputs, and repolarization of the membrane after action potentials. The activation kinetics of voltage-gated potassium

currents determines the rhythmic activity of neurons. Somewhat paradoxically, dampening of excitation is necessary for high frequency firing of neurons (Hille, 2001). The functional diversity of potassium channels reflects not only gene number, but also RNA editing, alternative splicing, post-translational modifications (e.g. phosphorylation, ubiquitination), channel modification by association with accessory subunits (Gutman et al., 2005; Li et al., 2006), and heteromeric assembly of sub-family members (Coetzee W.A et al., 1999). For an in-depth discussion of the molecular diversity of potassium channels, see Coetzee et al., 1999.

The K⁺ channel pore

Potassium channels favor potassium over sodium by a factor of 10^4 (Hille, 2001). The sequence/structure of the pore and the selectivity filter are highly conserved among all the varied family members (Miller, 2000). The selectivity for potassium is based on the signature sequence of amino acids GYG (Heginbotham et al., 1992; Heginbotham et al., 1994). This selective pore can conduct K⁺ ions at rates up to 10^8 ions per second, which approaches the conduction velocity of aqueous diffusion. The seeming paradox of this high selectivity with the remarkably high conduction rate was explained when the crystal structure of KcsA, a potassium channel from bacteria was solved (Doyle et al., 1998). Carbonyl oxygens of the GYG signature sequence are spaced

along the 12-Angstrom selectivity filter at perfect intervals for charge-charge interactions that fit the radius of potassium ions. Two K^+ ions fit in the pore simultaneously, and their electrostatic repulsion contributes to conduction velocity. With its smaller radius, Na^+ encounters a larger energy barrier to move from one interaction to the next. High sequence homology of both the pore and selectivity filter in all potassium channels indicates that this crystal structure accurately describes all superfamily members, a prediction that has held true (Long et al., 2005).

K^+ channel phylogeny based on trans-membrane topology

All potassium channels are complexes of subunits with four pore-forming domains required to form a pore. A channel can be assembled as a dimer of two subunits each with 2 pore-forming domains, or a tetramer of 4 subunits each with 1 pore-forming domain. The superfamily consists of three structural groups, based on their trans-membrane topology: 6TM 1P (6 transmembrane domains, 1 pore-forming domain), 2TM 1P, and 4TM 2P (**fig. 1**).

Figure 1. Dendrogram showing the three main groups (by membrane topology) of mammalian potassium channel alpha subunits, with 71 species. Image taken from Guman, G.A., Chandy, K.G., Adelman, J.P., Aiyar, J., Bayliss, D.A., Clapham, D.E., Covarrubias, M., Desir, G.V., Furuichi, K., Ganetzky, B., *et al.* (2003). International Union of Pharmacology. XLI. Compendium of voltage-gated ion channels: potassium channels. *Pharmacol Rev* 55, 583-586.

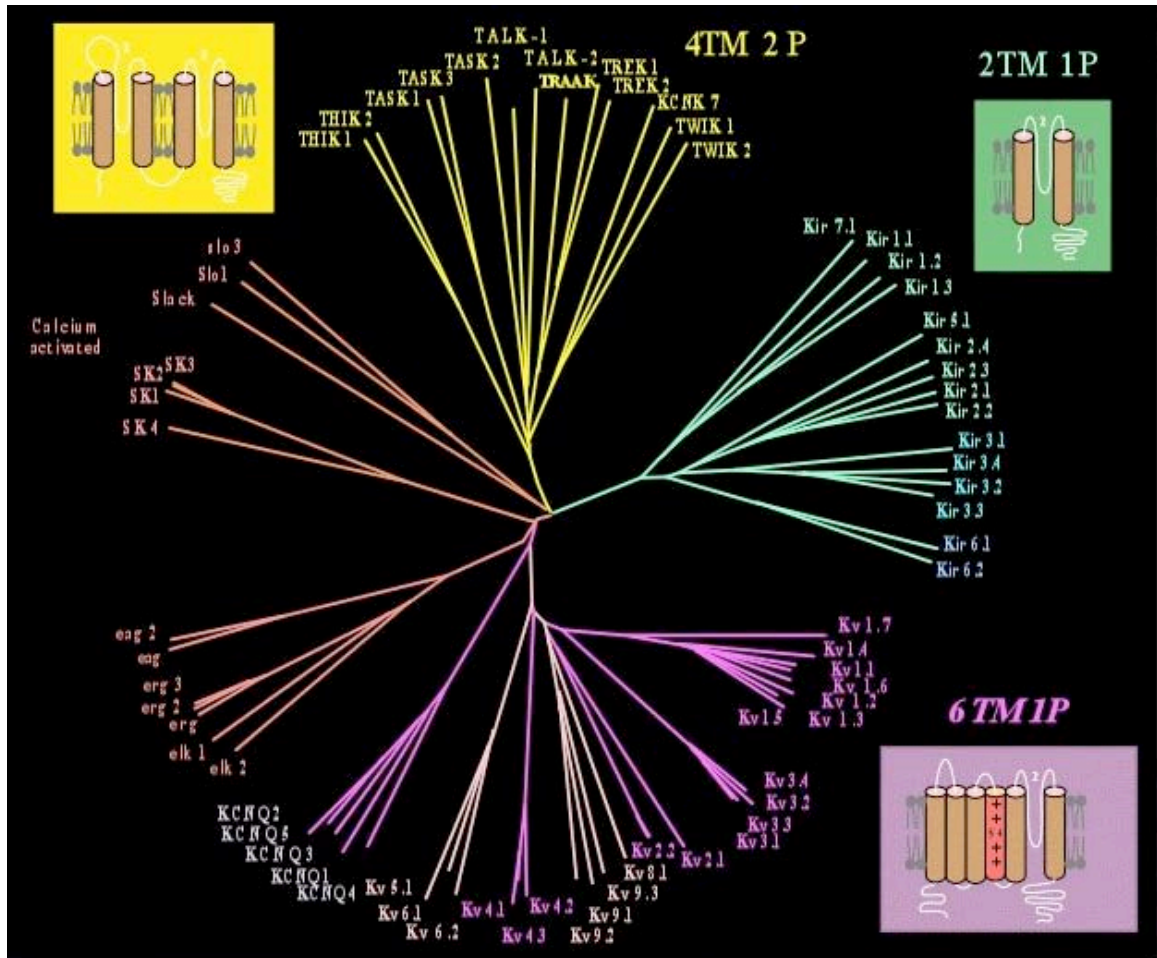


Figure 1.

2TM 1P subunits assemble as tetramers to form inwardly rectifying potassium channels (Kir), which allow inward K^+ currents at hyperpolarized potentials. Outward K^+ currents are blocked by intracellular polyamines, thus conferring the inward rectification. Kir channels regulate neuronal as well as non-neuronal signaling, including the heart rate (by controlling action potential duration in cardiac muscle), insulin release, and blood flow. This group includes the renal outer medullary potassium channels, G protein-coupled receptor-coupled K^+ channels, and ATP-sensitive members. **4TM 2P** subunits form dimers to achieve the necessary 4 pore-forming domains. These are classically known as the “leak” channels that contribute to maintenance of the resting membrane potential.

6TM 1P subunits comprise the largest family. These subunits form tetrameric structures, and can be subdivided into the voltage-gated potassium channels, and the voltage-insensitive calcium-activated potassium channels. Voltage-gated channels contribute to repolarization after action potentials. Inter-spike intervals are set, in part, by the kinetics of this repolarization, meaning that 6TM 1P channels in large part determine frequency of neuronal firing. Calcium-activated channels are themselves divided into 2 groups: large conductance (BK), and small conductance (SK). These two groups dampen excitability following calcium influx, which can manifest as negative feedback during excitatory postsynaptic potentials (EPSPs), or as the after-hyperpolarization (AHP) following action potentials (Coetzee et al., 1999). Two 6TM 1P potassium channels are central to

this thesis: Kv1.1-containing voltage-gated channels, and the small-conductance calcium-activated potassium channel SK2. Both of these channels play a role in cerebellar processing.

Cerebellar anatomy

The cerebellum (Latin for “little brain”) is a highly organized brain structure that is central to motor processing. The deep cerebellar nuclei in the interior of the cerebellum are wrapped in the white matter of the Purkinje cell axons that innervate them. The cerebellar cortex has three morphologically distinct layers (Fig. 2). The first layer (innermost to the white matter) is the granule cell layer. This layer is mostly composed of densely packed granule cells, numbering above 10^{10} in the human brain. Although the cerebellum accounts for 10 percent of the brain by weight, cerebellar granule cells account for more than half of the neurons in the entire nervous system. Two interneuron types, Golgi cells and Lugaro cells, are interspersed among the granule cells. The second layer of the cortex consists of Purkinje cell bodies, the principal cells of the cerebellum. The planar spread of Purkinje cell dendrites extends into the molecular layer, which is populated by basket and stellate interneurons, as well parallel fibers arising from granule cells.

Two major projections enter the cerebellum, both excitatory. Climbing fibers arise from the inferior olive carrying sensory information and feedback from the

cerebral cortex. Climbing fibers synapse onto the soma and dendrites of Purkinje cells, and elicit large depolarizations, resulting in complex spikes. Mossy fibers, like climbing fibers, convey both sensory information and feedback from the cerebral cortex. Mossy fiber projections arise from spinal cord and brainstem nuclei, and form excitatory synapses onto granule cell dendrites. Granule cells give rise to the parallel fibers. Parallel fibers project into the molecular layer, where they bifurcate and run longitudinally along the folia forming excitatory synapses onto Purkinje cell dendrites and molecular layer interneurons, basket cells and stellate cells. Basket cells form large, soma-engulfing presynaptic terminals onto Purkinje cells. The basket cell to Purkinje cell inhibitory synapse is a principal focus of this thesis. Finally, Purkinje cells project inhibitory contacts to the deep cerebellar nuclei. Purkinje cells are the sole output; their action potentials encode the sum total of processing in the cerebellar cortex. (Kandel, 2000; Manto and Pandolfo, 2002).

In addition to the main inputs from climbing and mossy fibers, the cerebellum receives aminergic input from nuclei in the brainstem: dopaminergic inputs arise from nucleus A10; noradrenergic inputs from locus ceruleus; and serotonergic inputs from the raphe nuclei. The noradrenergic inputs synapse onto distal Purkinje cell dendrites and basket cells, one function of which is addressed by experiments in chapter 2 of this thesis.

Figure 2. Lithograph plate detailing the synaptic connections of the cerebellar cortex. Transverse section of a cerebellar folium. (Diagrammatic, after Cajal and Kölliker.) Gray's Anatomy of the Human Body, 20th Ed. 1918.

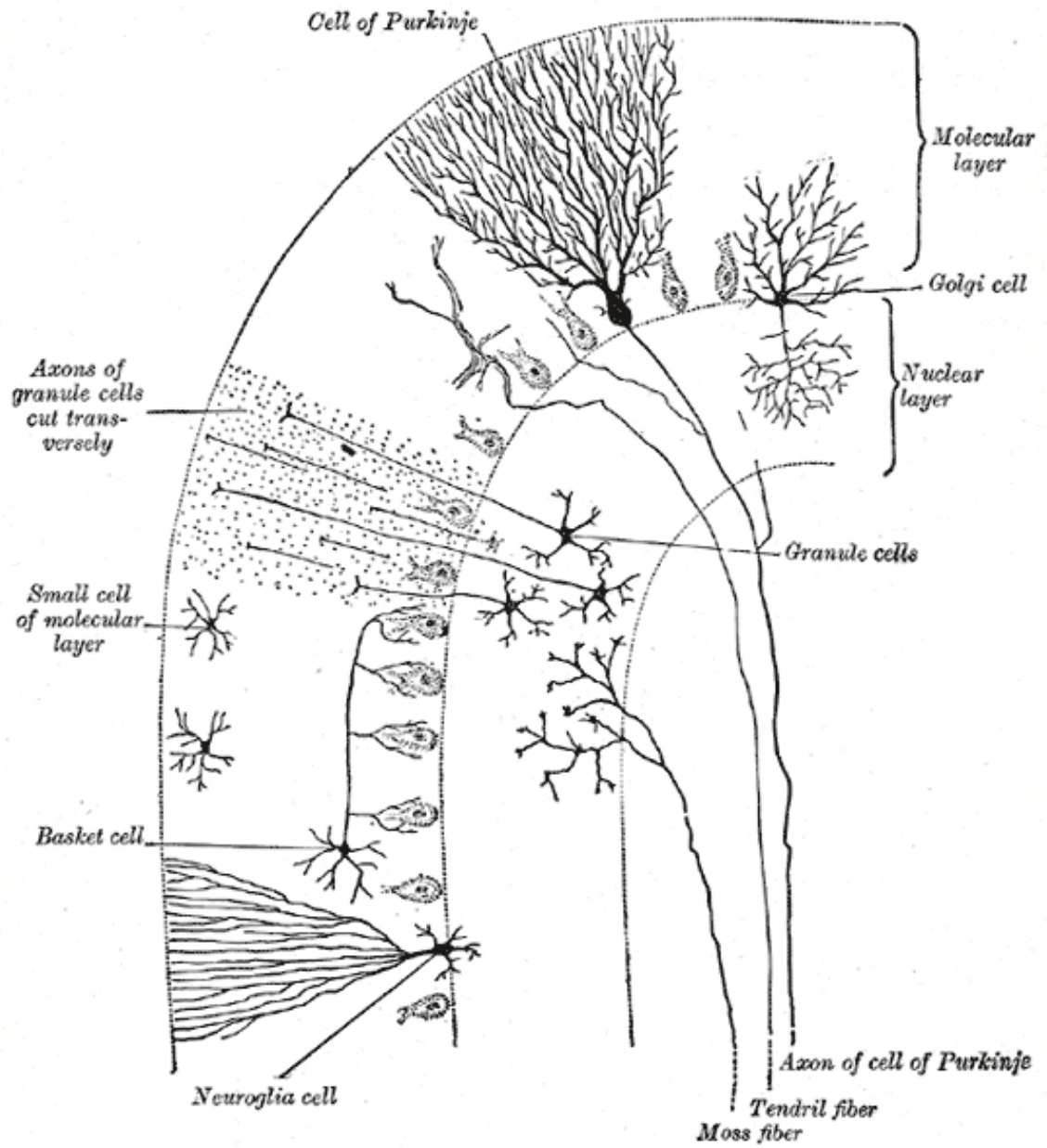


Figure 2.

Purkinje cells are intrinsic pacemakers

Brain activity has to start somewhere. Although most neurons require external stimulation to fire action potentials, a few types fire action potentials spontaneously, and are thus termed pacemakers. Many CNS neurons exhibit pacemaking, including cells of the locus coeruleus (Williams et al., 1984), thalamic neurons (Jahnsen and Llinas, 1984), and cells of the suprachiasmatic nucleus (Pennartz et al., 1997). Purkinje cells also exhibit intrinsic pacemaking. *In vivo* Purkinje cell recordings demonstrate regular, spontaneous action potentials (Bell and Grimm, 1969, Latham and Paul, 1971), which is maintained in cultured Purkinje cells (Gruol and Franklin, 1987; Raman and Bean, 1999) and in acute cerebellar slices (Hounsgaard, 1979; Llinas and Sugimori, 1980 (Hausser and Clark, 1997a), all in the presence or absence of synaptic transmission. Climbing fiber stimulation interrupts this tonic firing pattern, eliciting short bursts called complex spikes (Eccles et al., 1966; Eccles et al., 1967; Martinez et al., 1971).

The classic pacemaker cell, the cardiac myocyte, activates I_h during the hyperpolarization of the action potential undershoot. I_h activation then depolarizes the cell to approximately -50mV, activating T-type Ca^{2+} channels and the subsequent action potential. The depolarization deactivates I_h and activates K^+ channels, terminating the action potential and hyperpolarizing the membrane.

This hyperpolarization simultaneously removes inactivation of I_h and activates it again. This sequence of events repeats like the swing of a pendulum.

The unique pacemaker mechanism in Purkinje cells is a resurgent Na^+ current (Raman and Bean, 1997; Raman and Bean, 1999). Depolarization of Purkinje cells to +30mV, followed by repolarization to -40mV, results in a large, transient, inward current that is TTx-sensitive. The Na^+ channels responsible for the resurgent current are the same as those that underlie the rising phase of the action potential. Resurgent Na^+ currents allow Purkinje cells to fire action potentials at high frequencies. The cytoplasmic tail of the $\beta 4$ subunit of the Na^+ channel occludes the pore, inactivating the channel. This blocking peptide binds to a site on the alpha subunit when the membrane is depolarized precluding classical inactivation. After repolarization, the blocking peptide is released from the alpha subunits, allowing a resurgent current to begin anew. This inactivation mechanism results in a much shorter refractory period between action potentials, accounting for spontaneous regular firing and high frequency of firing (Raman and Bean, 1997) (Grieco et al., 2005).

The Bean laboratory, using trains of pre-recorded action potentials as voltage commands, in conjunction with ion substitution and selective blockers, elucidated the ionic currents underlying spontaneous activity in dissociated Purkinje cells (Raman and Bean, 1999). A current that maintains spontaneous action potentials would be expected to be prominent in the interspike interval. In their experiments,

as the membrane potential rose from -65 to -60 mV in their imposed spike trains, the predominant current was TTx-sensitive, and carried by Na^+ . Large voltage-dependent Ca^{2+} currents were observed during spiking. Rather than depolarizing the cell, the net effect of these Ca^{2+} currents was to hyperpolarize the cell by activating Ca^{2+} -activated potassium currents. Both T-type and P-type Ca^{2+} channels are expressed in Purkinje cells. T-type channels had a net depolarizing effect, as the specific blocker mibefradil decreased firing frequency by 30%, which implies that P-type calcium channels are the trigger for activation of calcium-activated potassium channels. Blocking all Ca^{2+} channels with cobalt did not stop firing in most neurons, but did reduce firing rate by 30% in their study. The voltage-gated potassium currents that repolarize the neuron after spikes deactivate quickly, pre-empting large hyperpolarizations, and re-establishing the input resistance necessary for the next spike. I_h was present, but was not necessary for modulating activity or firing rate. This lack of reliance on I_h distinguishes Purkinje cells from most other pacemakers.

Figure 3. Cell of Purkinje from the cerebellum. Golgi method. (Santiago Ramon y Cajal.) *a.* Axon. *b.* Collateral. *c* and *d.* Dendrons. Engraving. Gray's Anatomy of the Human Body, 20th Ed. 1918.



Figure 3.

Synaptic modulation of Purkinje cell output

Basket cell interneurons fire spontaneously *in vivo* and *in vitro*, providing a basal level of inhibitory tone in Purkinje cells. Acutely dissociated Purkinje cell preparations, such as those used to investigate the pacemaker mechanism, lack dendrites and synaptic inputs. Isolated Purkinje cells fire faster (50 Hz vs. 40 Hz), possibly because they lack inhibitory GABAergic input. In agreement with this idea, the firing frequency of dissociated Purkinje cells is similar to Purkinje cells in slice experiments in the presence of the GABA_A receptor blocker picrotoxin. Purkinje cells summate all excitatory and inhibitory activity in cerebellar cortex and provide its sole output. Information from the cerebellar cortex is conveyed not only through the constant rate of Purkinje cell firing but also, and perhaps more importantly, through rate and mode changes. The spontaneous regular firing of Purkinje cells allows for bi-directional modulation by excitatory and inhibitory contacts. Bidirectional modification allows for faster encoding of the time-variant information from cortical and sensory inputs (Eccles, 1973).

The cerebellar ataxias

The cerebellum is required for motor coordination, and damage to the cerebellum can result in severe motor deficits. Much of what we know about cerebellar function has been defined by what goes wrong when it fails. The main motor signs of cerebellar dysfunction are tremor associated with intentional

movements, and ataxias. The cerebellar ataxias comprise a class of debilitating diseases that disrupt motor coordination and movement. Ataxias can result from genetic mutation, as well as physical lesions, toxic insult, or mis-regulated development of the cerebellum.

Many hereditary ataxias result from mutations in ion channel genes, although the biophysical effects of the mutation and underlying cellular mechanisms are only partially understood. The cerebellar disorder episodic ataxia/myokymia type 1 (EA1) maps to KCNA1, and Episodic ataxia type 2 (EA2) results from mutations in P/Q-type voltage-gated Ca^{2+} channel genes. These channelopathies can tell us much about the function of the cerebellum, and the role of K^+ channels in cerebellar processing.

Episodic ataxia/myokymia type 1

EA1 is an inherited autosomal dominant neurological disorder characterized by attacks of uncontrolled movements and imbalance (Ashizawa et al., 1983). Attacks can be induced by both physical and emotional stress. These attacks are ameliorated in many individuals by the carbonic anhydrase inhibitor acetazolamide, although its mechanism of action is not known. Attacks last a matter of minutes, and can occur multiple times per day (Gancher and Nutt, 1986). Symptoms and responses to treatment vary both between and within families.

EA1 has been linked to missense and, in one case, nonsense, point mutations in KCNA1, the gene that encodes the voltage-gated delayed rectifier potassium channel subunit Kv1.1 (Browne et al., 1994; Litt et al., 1994; Browne et al., 1995). KCNA1 is the mammalian homolog of the *Drosophila* gene Shaker, the first cloned potassium channel gene (Tempel B.L. et al., 1987). Shaker mutant flies demonstrate a loss of motor control phenotype: shaking legs during the period immediately following ether anesthesia. Similarly, a single missense point mutation in KCNA1 causes loss of motor control in EA1 patients during stress.

EA1 mutations are scattered throughout the Kv1.1 protein, but occur at evolutionarily conserved positions in KCNA1 (Litt et al., 1994; Browne et al., 1995; Comu et al., 1996; Zuberi et al., 1999; Lee et al., 2004). Some EA1 mutations, including F249I, reduce surface expression of the protein, and are thought to confer disease through haplo-insufficiency. However, most EA1 mutant subunits form functional channels. All of the EA1 mutations reduce current amplitudes, reflecting a loss of function of Kv1.1 containing voltage gated K⁺ channels. This reduction results from various biophysical alterations among the different familial mutations. For example, E325D mutants cause right-shifted voltage-dependence of activation, resulting in reduced activation at physiological membrane voltages. Other mutants cause unstable open states, or altered kinetics of activation, deactivation, or inactivation. (Adelman et al., 1995; Comu et

al., 1996; Zerr et al., 1998b, a; Zuberi et al., 1999; Maylie et al., 2002a) (Figure 4).

The mutation most carefully considered in this thesis is V408A, which resides on the cytoplasmic end of S6 flanking the pore domain. The unstable open state of homomeric V408A channels expressed in oocytes causes a 10-fold increase in the deactivation rate (Adelman et al., 1995), as well as alterations of inactivation kinetics (Maylie et al., 2002a).

All EA1 patients are heterozygous for their particular familial mutation in KCNA1, suggesting that homozygous mutations are lethal. Expressed mutant Kv1.1 subunits have a dominant negative effect through co-assembly with WT subunits to form the many possible configurations of Kv1.1 channels. These heteromeric channels typically display biophysical profiles that are intermediate between homomeric mutant and homomeric wild type channels (Zerr et al., 1998b; Maylie et al., 2002b). Kv1 channels are divided into seven subfamilies based upon primary sequence homology and the ability to form heteromeric channels with other Kv1 family subunits. Kv1 channel diversity of function results in large part from these heteromeric combinations, and is amplified by association with various beta subunits. Although much of the work describing the biophysical consequences conferred by EA1 mutations is based on homomeric expression studies, Kv1.1 subunits are predominantly if not

Figure 4: Topographical illustration of the known familial EA1 mutations within the Kv1.1 subunit. Four such subunits combine to form functional K⁺ channels.

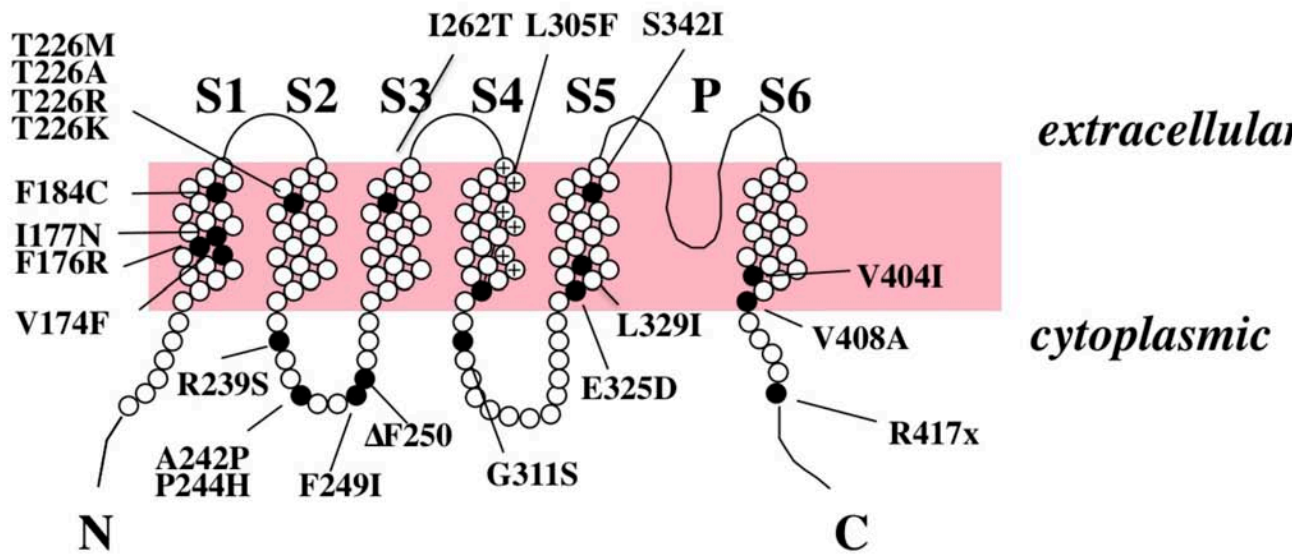


Figure 4

always incorporated into heteromeric channels *in vivo* (Coleman et al., 1999). Kv1.1 typically forms heteromeric complexes with other Kv1 family members, particularly 1.2, 1.4, and 1.6. Like the co-expression of mutant Kv1.1 with WT Kv1.1, the effects of the EA1 mutations are conferred in a dominant negative fashion onto all the heteromeric channels that can be formed with other Kv1 subunits.

The ramifications of all stoichiometric combinations are difficult to predict. The unstable open states might result in reduced ability of mutant subunit-containing channels to contribute to the establishment of resting potential and/or action potential re-polarization. This could lead to prolonged action potentials, increased Ca^{2+} influx, and increased neurotransmitter release. To study the ramifications of the loss of function mutations in whole animals, the Adelman and Maylie laboratories inserted the V408A mutation into the mouse genome by homologous recombination. The resulting mouse model of EA1 recapitulates the key aspects of the disease: Stress induction of the ataxic phenotype, and acetazolamide amelioration (Herson et al., 2003). This mouse model can be used to determine how a single point mutation in KCNA1 can confer a stress-induced motor deficit.

+V408A Purkinje cells receive increased GABAergic input

Basket cells contribute the main GABAergic input to Purkinje cells at large axo-somatic contacts (Ito, 1984). This architecture suggests that basket cells have great influence over the ultimate output of the cerebellar cortex. Immunohistochemistry and *in situ* hybridization data, as well as direct electrophysiological recordings from presynaptic terminals, show that Kv1.1 channels (and hence the V408A mutation) are heavily expressed in the basket cell synaptic terminals and axonal branch points, but are not expressed in the Purkinje cells (Fig. 5) (Tsaur et al., 1992; Wang et al., 1994; Southan and Robertson, 1998).

Figure 5. Top, Kv1.1 reaction product in the Purkinje cell layer of the cerebellar cortex. Bottom, Kv1.1 expression is restricted to basket cell presynaptic terminals that surround Purkinje cells. Kv1.1 is not expressed postsynaptically in Purkinje cells. Immunohistochemistry and transmission electron micrographs by Wang et al., 1994.

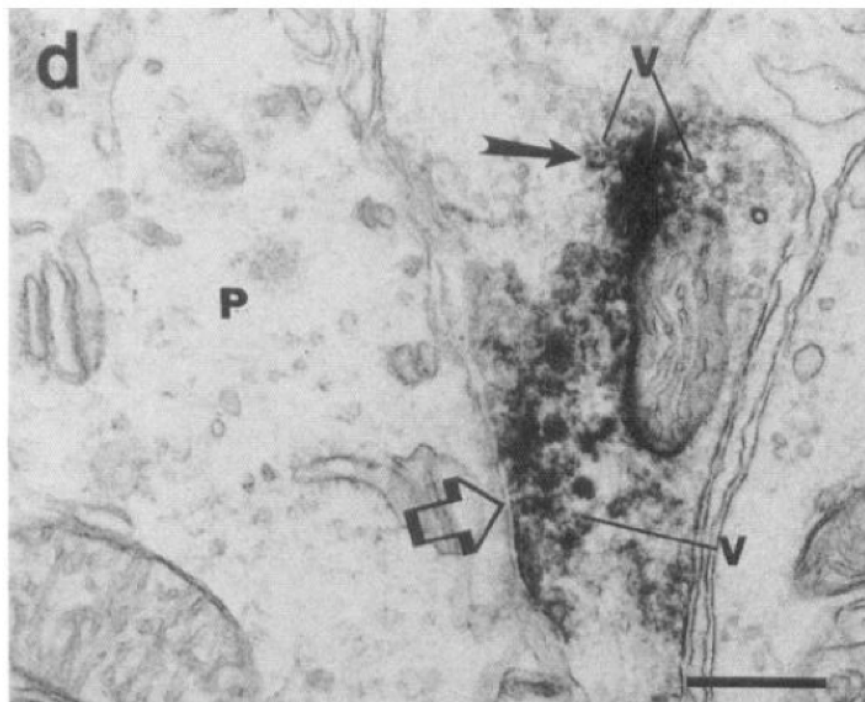
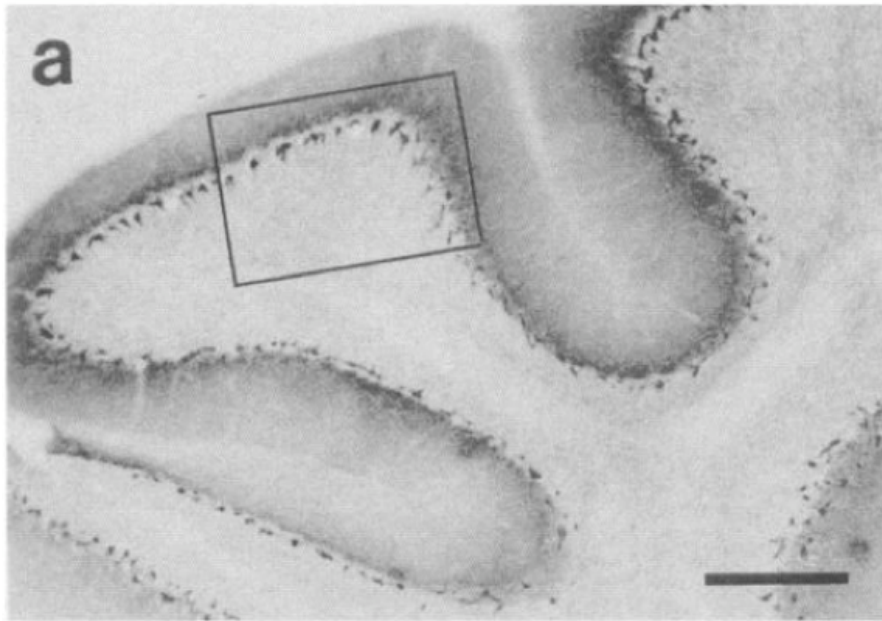


Figure 5.

This expression pattern, and the decreased repolarizing activity in cells expressing EA1 mutant channels, could cause basket cells to release more GABA. Consistent with this idea, GABAergic synaptic currents in +V408A Purkinje cells have a higher frequency and average amplitude (Herson et al., 2003). A principal goal of this thesis was to determine whether increased GABAergic inhibition of Purkinje cells contributes to the motor-coordination deficit in EA1.

β -adrenergic stress further increases inhibitory tone in Purkinje cells

Isoproterenol, a potent synthetic agonist of β -adrenergic receptors (β -AR), is required to trigger stress-induced motor deficits in +V408A mice. This adrenergic stress is a model of emotional stress, which induces ataxia in EA1 patients. Axonal projections from the locus ceruleus provide diffuse noradrenergic innervation to the cerebellar cortex (Olson and Fuxe, 1971; Ungerstedt, 1971). Noradrenaline signaling from these inputs has long been known to potentiate GABA_A receptor-mediated inhibition of Purkinje cell firing (Hoffer, 1971; Waterhouse, 1982), by eliciting long-term facilitation of GABAergic transmission onto Purkinje cells. Activation of basket cell β -ARs increases cAMP levels through adenylate cyclase activation. cAMP binds directly to HCN-1 channels and shifts the hyperpolarization-activated cation channel (I_h) voltage dependence of activation to more positive potentials, making smaller hyperpolarizations

sufficient to open I_h channels, resulting in depolarization of presynaptic terminals and increased transmitter release (Saitow and Konishi, 2000; Saitow et al., 2000). This results in an increase in frequency (Llano and Gerschenfeld, 1993) and amplitude of basket cell-mediated inhibitory postsynaptic currents (IPSCs) (Saitow et al., 2000). Such an increase in inhibitory tone can depress the output of the cerebellar cortex (Mitoma and Konishi, 1996, 1999). Through this mechanism, adrenergic stress is predicted to increase GABAergic signaling, similar to the EA1 mutation V408A. During adrenergic stress, these two sources of GABAergic increase would be expected to summate, a prediction we tested.

Pacemaking precision deficits in ataxia

The enhancement of GABAergic transmission could affect the regularity, or “precision” of Purkinje cell firing. The coefficient of variation of the inter-spike interval (CV_{ISI}), defined as $Standard\ Deviation_{ISI}/Mean_{ISI}$, provides an index of firing irregularity normalized to the firing rate. Basal GABAergic transmission influences Purkinje cell firing in rats. GABA contributes to the irregularity of the interval, i.e. increases CV_{ISI} , and slows frequency of firing (Hausser and Clark, 1997a).

Episodic ataxia type 2 (EA2) is linked to mutations that affect P/Q-type voltage-gated calcium channels (VGCC) or their auxiliary subunits (Pietrobon, 2002). Three motor-impaired mouse models of EA2 exhibit reduced regularity of

Purkinje cell inter-spike intervals (Hoebeek et al., 2005; Walter et al., 2006). *Leaner* mice have a spontaneous mutation in CACNA1, which encodes the α_{1A} subunit. *Ducky* mice have a spontaneous mutation in CACNA2d2, which encodes the $\alpha_{2\delta 2}$ auxiliary subunit. Both mutations decrease P/Q-type calcium current density. In the study by Walter, Alvina et al., Purkinje cell firing rates in *ducky* and *leaner* mice had three-fold the interspike interval variation of WTs. Parallel fiber stimulations evoked discernable increases in firing rates of WT Purkinje cells, but the increases were not discernable from the background variation in *ducky* and *leaner*. The reduced signal to noise ratio suggests that reduced fidelity of synaptic encoding causes motor deficits in P/Q-type calcium channel mutants (Walter et al., 2006).

In partial summary, +/V408A Purkinje cells receive increased GABAergic input. β -AR activation further increases GABAergic transmission in WT Purkinje cells, and is required to elicit a motor deficit in +/V408A mice. GABAergic input contributes to imprecision of the interspike interval, and imprecision of the interspike interval underlies motor deficits in a related ataxia.

Based on these results, I examined whether +/V408A Purkinje cells have a firing precision deficit, and whether this deficit is a result of increased GABAergic transmission from BCs. I studied +/V408A Purkinje cell firing patterns in acute cerebellar slices with synaptic inhibition intact. In chapter two I show that +/V408A Purkinje cells had reduced precision of spontaneous action potential

firing, and that this difference was due to increased GABAergic input. Activation of β -adrenergic receptors exacerbated the +/V408A precision deficit, and acetazolamide ameliorated it. Together, these data suggest that the precision deficit in +/V408A Purkinje cells is the cellular basis for the motor deficit in EA1.

SK2 and Purkinje cell firing patterns

In the section above, I described the importance of regularity of Purkinje cell interspike intervals, and the importance of this regularity for motor coordination. Much of the evidence for this relationship involves calcium-activated potassium channels such as SK2. SK channels are activated by increases in intracellular Ca^{2+} ($\text{IC}_{50} = 300\text{-}700$ nM), and are voltage insensitive. Sources of calcium activation include voltage-gated calcium channels, calcium permeable ligand-gated channels, and intracellular Ca^{2+} stores. Ca^{2+} sensitivity is conferred by calmodulin, a subunit that is constitutively bound to the C-terminal region of each SK subunit (Xia et al., 1998). Much of our understanding of SK function results from the use of pharmacological agents, such as apamin, EBIO, and NS309. SK channels are specifically blocked by apamin, a peptide derived from honey bees (*Apis mellifera*) (Chen et al.; Blatz and Magleby, 1986). Activators that enhance SK channel Ca^{2+} sensitivity include NS309 and 1-ethyl-2-benzimidazoline (EBIO) (Pedarzani et al., 2001; Strobaek et al., 2004).

SK channels have a variety of functions in central neurons. SK channels contribute to the afterhyperpolarization (AHP) that follows action potentials, and regulate synaptic plasticity by forming a negative feedback loop with NMDA receptors in dendritic spines (Ngo-Anh et al., 2005). SK channels generally dampen postsynaptic excitation, and control dendritic integration (Cai et al., 2004).

Of the four mammalian SK channels, only SK1-3 are expressed in neurons (Sailor et al., 2004). Encoded by the KCNN gene family, these three channels were cloned in the Adelman laboratory in 1996 (Kohler et al., 1996). Knock-out mice have been generated for each of these genes (Bond et al., 2004). SK3 channels affect parturition and respiration in mice (Bond et al., 2000). SK2 channels contribute afterhyperpolarizing (AHP) currents in hippocampal CA1 neurons (Bond et al., 2004). No phenotype or function has yet been reported for SK1.

Disruption of a Ca^{2+} -activated K^+ channel causes irregular Purkinje cell firing and motor deficits

Mice lacking large conductance Ca^{2+} activated potassium channels (BK) display intention tremor, gait abnormalities, and impaired conditioned eye-blink reflexes, well as performance deficits on rotarod and balance beam. A high proportion of Purkinje cells in $\text{BK}^{-/-}$ mice are silent, and those that fire action

potentials have reduced tonic firing. Without the contribution of BK to the fast AHP, interspike intervals are longer. The absence of BK also leaves the membrane relatively depolarized following the action potential, inducing inactivation of Na⁺ channels (Sausbier et al., 2004).

Disruption of a voltage-gated Ca²⁺ channel decreases precision and causes motor deficits

Episodic ataxia type 2 results from mutations in CACNA1, which encodes P/Q-type voltage-gated calcium channels, and reduces Ca²⁺ current density (Wakamori et al., 1998; Pietrobon, 2002). The spontaneous P/Q-type calcium channel mutation in mice, *tottering*, also displays disrupted regularity of Purkinje cell simple spikes in the flocculus during optokinetic stimulation. The altered gain and phase of compensatory eye movements in *tottering* are equal to mice after removal of the flocculus, indicating that this loss of pacemaking precision is tantamount to removal of the cerebellar circuit necessary for this motor task (Hoebeek et al., 2005). Because mutations in CACNA1 result in human ataxia, this work suggested that decreased precision of Purkinje cell pacemaking might underlie motor deficits. Because P/Q channels are coupled to SK channels in Purkinje cell dendrites, one possibility is that the phenotype of CACNA1 mutations results from reduced SK channel activity (Womack et al., 2004).

Support for this idea was provided by experiments with EBIO, which increases SK2 activation by increasing the apparent calcium sensitivity of SK channels

(Strobaek et al., 2004). The motor deficits and dyskinesia of *tottering* mice were partially reversed by *in vivo* EBIO perfusion, indicating that one consequence of reduced P/Q type Ca^{2+} current density is reduced activation of SK channels. The P/Q-type mutants *ducky* and *leaner*, were used to investigate the connection between calcium activation of SK2, Purkinje cell firing regularity, and motor coordination. The AHP amplitude was reduced in slice recordings of *ducky* Purkinje cells, and was restored by EBIO. EBIO similarly restores firing precision in *leaner* and *ducky* Purkinje cells, as well as ameliorating the motor deficits of *ducky* similarly to *tottering* mice (Walter et al., 2006). Recently, *tottering* motor deficits were relieved by oral administration of Chlorzoxazone, a FDA-approved activator of calcium-activated potassium channels (Alvina and Khodakhah, 2010). As a result of this work, the following model was proposed: reduced Ca^{2+} current density due to mutations in P/Q-type Ca^{2+} channels (or their auxiliary subunits) provides insufficient activation of SK2, resulting in a reduced AHP amplitude. This causes irregular Purkinje cell pacemaking, which results in ataxia, possibly due to reduced fidelity of synaptic encoding in Purkinje cells (Figure 6). This model suggests that any reduction of SK2 activity, where P/Q type calcium channels are also expressed, would phenocopy episodic ataxia type 2.

Figure 6. A proposed mechanism by which VGCC-related mutations cause ataxia. Reduced Ca^{2+} current density due to mutations in P/Q-type Ca^{2+} channels (or their auxiliary subunits) is insufficient for normal SK2 activation. This causes irregular Purkinje cell pacemaking, possibly as a result of reduced AHP amplitude, and results in ataxia. The irregular firing behavior and the accompanying ataxia are reversed by EBIO. (Figure from Otis and Jen, 2006, a News and Views article regarding (Walter et al., 2006))

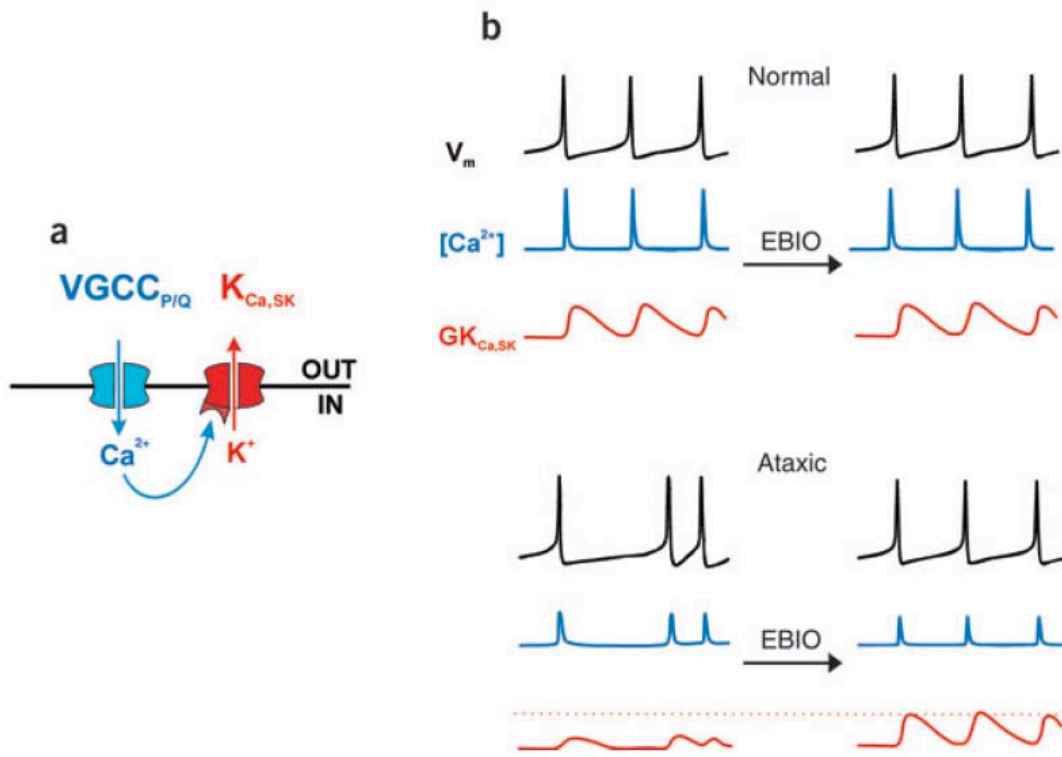


Figure 6.

The results of the EA2 mouse model experiments suggest that reducing SK channel activity in Purkinje cells should cause irregular Purkinje cell pacemaking and motor deficits. Of the three mammalian SK subunits expressed in central neurons, only SK2 is expressed in Purkinje cells (Cingolani et al., 2002; Womack and Khodakhah, 2003), thus making SK2 the target of our experiments. Both somatic and dendritic SK2 channels contribute to control of action potential firing in Purkinje cells. The SK-specific channel blocker apamin increases Purkinje cell firing frequency in acute cerebellar slices, and transforms tonic firing to burst firing (Womack and Khodakhah, 2003). Thus, in chapter 3, I examined intrinsic Purkinje cell firing precision and motor coordination in a mouse model of reduced SK2 expression: homozygous floxed SK2 mice ($SK2^{fl/fl}$) (Bond et al., 2004). Recordings were performed from acute cerebellar slices with fast synaptic transmission blocked. $SK2^{fl/fl}$ mice had regular Purkinje cell pacemaking in only 2 lobules (VIII and IX) of the cerebellum, and yet showed no overt motor deficit. Ablation of lobules VIII and IX in $SK2^{fl/fl}$ mice removes the only region of regularly firing Purkinje cells in their vermis, and reduced their performance on the balance beam. Ablation of lobules VIII and IX had no effect on WT performance on the balance beam. This result supports the notion that Purkinje cell pacemaking is required for cerebellar-dependent motor tasks. Conversely, ablations did not impact $SK2^{fl/fl}$ ability on the accelerating rotarod, indicating that this mouse line

does not require regular Purkinje cell firing in the vermis to perform this assay. This result suggests that the balance beam and rotarod have differing dependence on Purkinje cell pacemaking, or that compensation occurs in the SK2^{fl/fl} animals.

Chapter II

The cellular basis of episodic ataxia type 1

Abstract

The dominant neurological disorder episodic ataxia type 1 (EA1) causes stress-induced ataxia, and results from mutations in the KCNA1 gene, which codes for the voltage-gated potassium channel Kv1.1. We examined firing patterns of cerebellar Purkinje cells in a mouse model of EA1 using acute brain slices. Purkinje cells received increased GABAergic input from basket cell interneurons that express Kv1.1 subunits. This increased GABAergic tone reduced the precision of Purkinje cell pacemaking, measured as a higher coefficient of variation of the interspike interval (CV_{ISI}). To mimic stress, we bath-applied the β -adrenergic agonist isoproterenol, which also increased the CV_{ISI} in EA1 and WT Purkinje cells in a GABAergic-dependent manner. The carbonic anhydrase inhibitor acetazolamide, which minimizes the frequency and severity of attacks in EA1 patients, reduced the CV_{ISI} in EA1 Purkinje cells back to WT levels. Pre-treating EA1 cerebellar slices with acetazolamide reduced the isoproterenol effect on CV_{ISI} , resulting in a value similar to that of WT in isoproterenol. These data are consistent with the hypothesis that a disruption of Purkinje cell firing represents the cellular basis of EA1.

Introduction

Balance, posture, and coordination are dependent on cerebellar function, thus mutations that affect cerebellar processing can cause tremor and ataxia (Kullmann, 2002). Cerebellar Purkinje cells integrate inputs from many regions and cell types, and are the sole output of the cerebellar cortex. Thus Purkinje cell signaling is required for motor planning, movement execution, and coordination (Ito, 1984). Cerebellar Purkinje cells fire action potentials spontaneously *in vivo* (Bell and Grimm, 1969; Shin et al., 2007) and *in vitro* (Hounsgaard, 1979; Llinas and Sugimori, 1980; Hausser and Clark, 1997b; Edgerton and Reinhart, 2003; Womack and Khodakhah, 2004). Purkinje cell firing shows a high degree of precision (Hausser and Clark, 1997a). Reduced precision of the inter-spike interval of Purkinje cells is associated with a motor deficit in two mouse models of episodic ataxia type 2 (Walter et al., 2006).

Episodic ataxia type1 (EA1) is a dominant neurological disorder characterized by attacks of imbalance and loss of motor control, which are induced by physical or emotional stress (Gancher and Nutt, 1986; Brunt and van Weerden, 1990; Browne et al., 1994). Many EA1 patients respond favorably to treatment with the carbonic anhydrase inhibitor acetazolamide, which minimizes the frequency and severity of attacks in EA1 patients (Gancher and Nutt, 1986). EA1 is caused by mutations in KCNA1, which codes for the voltage-gated potassium channel Kv1.1 (Browne et al., 1994). Each affected family carries a different point mutation in

the Kv1.1 gene and all affected individuals are heterozygous. We previously inserted a known EA1 mutation, V408A, into the mouse genome by homologous recombination (Herson et al., 2003). Heterozygous +/V408A mice show stress-induced impairment of motor coordination that is precluded by acetazolamide, and therefore these mice recapitulate the two key behavioral phenotypes of the human disease.

Basket cells contribute the main GABAergic input to Purkinje cells at large axo-somatic contacts (Ito, 1984). This architecture suggests that basket cells greatly influence the output of the cerebellar cortex. Kv1.1 is expressed in the presynaptic terminals of basket cells (Wang et al., 1993; Wang et al., 1994), and the V408A mutation results in increased GABA release from these terminals, reflected by a higher frequency and amplitude of spontaneous GABAergic inhibitory postsynaptic potentials in Purkinje cells (Herson et al., 2003). Blocking Purkinje cell GABA_A receptors with picrotoxin reduces the coefficient of variation of the inter-spike interval, demonstrating that GABAergic signaling contributes to imprecision (Hausser and Clark, 1997a).

We tested the hypothesis that increased GABA release from EA1 basket cells alters the output of Purkinje cells and contributes to the motor-coordination deficit in EA1. We studied +/V408A Purkinje cell firing patterns in acute cerebellar slices with synaptic inhibition intact. +/V408A Purkinje cells had reduced precision of spontaneous action potential firing, because of increased GABAergic input.

Activation of β -adrenergic receptors exacerbated this deficit, and acetazolamide ameliorated it. Together, these data suggest that the firing precision deficit of EA1 Purkinje cells underlies the motor deficit in EA1.

Methods

Cerebellar slice preparation. Sagittal cerebellar slices (300 μ M thick) were prepared from WT C57BL/6J mice (8-12 week) and +/V408A littermates as previously described. Procedures were consistent with institutional safety and IACUC guidelines. Briefly, mice were first sedated by intraperitoneal injection of a ketamine/xylazine mixture, and then perfused through the left ventricle with ice-cold oxygenated ACSF solution described below. Following decapitation, the cerebellum was removed and sagittal slices of the vermis cut on a Leica VT1000s (Leica Instruments, Nussloch, Germany). Slices were incubated in ACSF at 35 °C for 30 min and then stored in ACSF at room temperature until used for recordings. Slices mounted in a chamber were perfused continuously with ACSF (2 ml/min) containing 5 μ M NBQX to block AMPA-type glutamate receptors and bubbled with a 95% O₂/5% CO₂ gas mixture. All experiments were performed at 35 °C within 4-5 hours of completion of slicing in order to ensure viability.

Solutions. The composition of the ACSF solution was (mM): 119 NaCl, 2.5 KCl, 1 NaH₂PO₄, 26.2 NaHCO₃, 1.3 MgCl₂, 2.5 CaCl₂, 10 Dextrose, and aerated with 95% O₂/5% CO₂.

Electrophysiology and analysis. Extracellular recordings were made from Purkinje cell somas visualized with infrared DIC on a Leica DMLFS upright microscope (Leica Microsystems, Wetzlar, Germany). Extracellular recordings were made in current clamp configuration using a Heka EPS10 amplifier (Axon Instruments, Union City, CA) interfaced to a Macintosh G4 (Apple, Cupertino, CA). Data was collected at a sample frequency of 10 kHz and filtered at less than 33% of the sampling frequency using Patchmaster (Heka Instruments Inc, Bellmore NY) and analyzed using macros written in Igor (Wavemetrics, Portland, OR).

All data are expressed are reported as mean \pm SEM, except where noted to be \pm SD. Comparisons were made by paired and unpaired t-tests as appropriate. Results were considered to be statistically significant when $P < 0.05$, or lower where noted. All significant results are designated.

Results

Purkinje cell firing precision in +V408A mice

To test whether the increased GABAergic tone alters action potential firing precision in Purkinje cells from +V408A mice, we made extracellular recordings of spontaneous Purkinje cells action potentials in acute cerebellar slices from the vermis of +V408A and WT mice. Fast glutamatergic transmission was blocked with DNQX (40 μ M) and firing precision was determined from the coefficient of variation (CV) of the interspike intervals, ISI, (CV_{ISI}). Representative recordings of extracellular action potentials from a WT and +V408A Purkinje cell are shown in **Fig. 1. 1A,D**. +V408A Purkinje cells displayed visibly reduced firing regularity compared to WT, as indicated by the hash marks above each trace and the plot of instantaneous firing frequency (**Fig. 1A**). Histograms of the ISI were more widely distributed in +V408A Purkinje cells compared to WT (**Fig. 1B,E**). A Gaussian distribution reasonably described each histogram. For comparison, the Gaussian fit for WT is superimposed on the +V408A histogram (**Fig. 1E**). The average CV_{ISI} for WT Purkinje cells was $CV_{ISI} = 0.073 \pm 0.005$, $n=50$; compared to $CV_{ISI} = 0.110 \pm 0.009$, $n=48$ in +V408A; $P<0.001$) (**Fig. 1C**). Consistent with increased GABAergic signaling, +V408A Purkinje cells also fired slower than WT Purkinje cells (WT frequency = 38.6 ± 1.7 Hz, $n=50$. +V408A frequency = 31.3 ± 1.5 Hz, $n=48$; $P<0.01$) (**Fig. 1F**).

Figure 1. Firing precision of WT and +V408A Purkinje cells. *A*, Representative extracellular recordings of action potentials from a WT Purkinje cell (middle trace) with idealized detected spikes plotted as hash marks (top trace). Instantaneous firing frequency (lower trace) plotted versus time. *B*, Probability histogram of the interspike intervals (ISI) measured from a one minute recording period from the cell shown in *A*. The histogram was derived from a total of 2145 events. The data were fit with a Gaussian distribution (dashed line) yielding a mean ISI of $27.08 \text{ ms} \pm 1.62 \text{ ms}$, $\text{CV} = 0.06$. *D-E*, Representative data from +V408A mice as described in *A-B*. The histogram was derived from a total of 1884 events. Mean ISI determined from Gaussian fit in *E* was $30.9 \text{ ms} \pm 3.4 \text{ ms}$, $\text{CV} = 0.11$. For comparison the Gaussian fit for WT in panel *B* is superimposed in Panel *E*, dotted line. *C*, Summary of CV data from all recordings. *** indicates $p < 0.001$. *F*, Summary of frequency of Purkinje cell firing from all recordings. ** indicates $p < 0.01$.

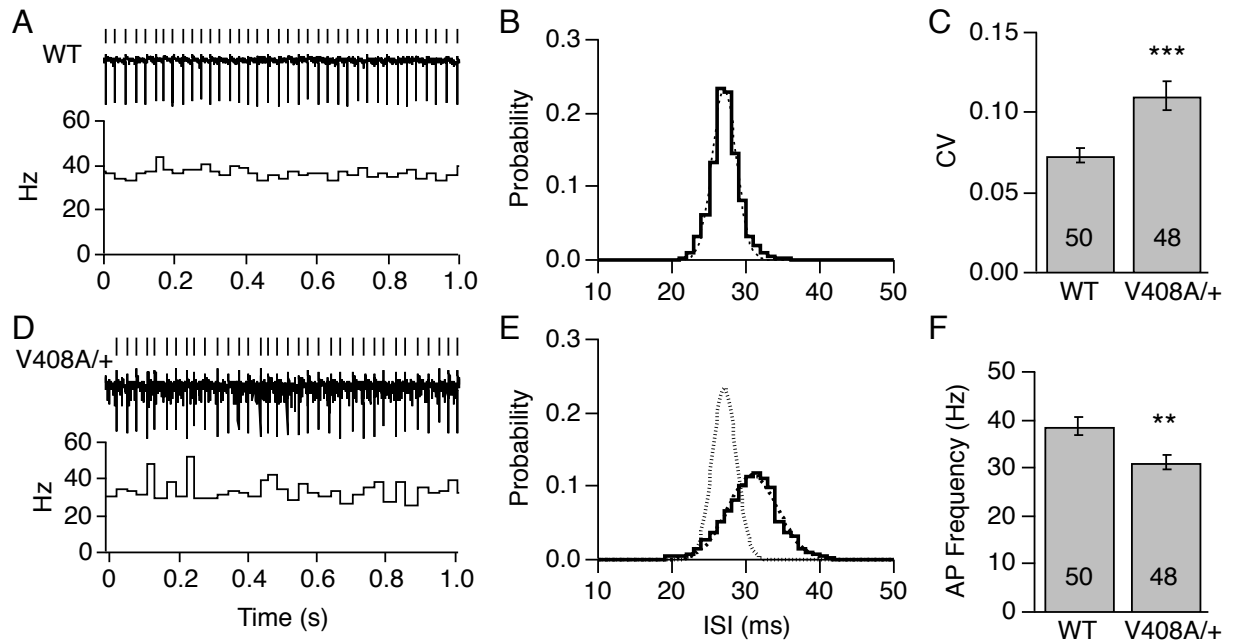


Figure 1.

Blocking GABA_A receptors occludes the +V408A deficits in precision and firing frequency

To evaluate the effects of GABAergic inhibition on firing patterns, slices were pre-incubated in picrotoxin (PTX, 50 μ M) for 30 minutes at room temperature prior to recording. In PTX, WT CV_{ISI} was 0.034 ± 0.011 , n=39, 46.8% of untreated WT CV_{ISI} ($P<0.001$). Similarly, in PTX +V408A CV_{ISI} was 0.034 ± 0.009 , n = 18 (**Fig.2A**), 32.6% of untreated +V408A CV_{ISI} ($P<0.001$). Thus, the CV_{ISI} in +V408A Purkinje cells was not higher than WT when GABA_A receptor-mediated transmission was blocked($P=0.661$).

Blocking GABA_A receptors with PTX increased the firing rate of +V408A Purkinje cells from 31.3 ± 1.5 Hz (data from **Fig. 1**) to 47.7 ± 4.4 Hz in PTX (n=18; $P<0.001$) (**Fig. 2B**). In contrast, blocking GABA_A receptors in WT Purkinje cells did not affect firing frequency (control = 38.6 ± 1.7 Hz (data from **Fig. 1**); PTX = 41.67 ± 2.3 Hz, n=39; $P=0.38$) (**Fig. 2B**). When GABAergic transmission is blocked, the two genotypes did not differ in either CV_{ISI} ($P=0.66$) or frequency ($P=0.29$).

Figure 2. GABAergic signaling accounts for genotypic difference in action potential firing precision in Purkinje cells. *A*, Bar graph of CV, control data recapitulated from **Fig. 1**. *B*, Bar graph of frequency of firing, control data recapitulated from **Fig. 1**. * indicates differences between genotypes in the same condition. † indicates differences between control and PTX treatment within a genotype. Data presented as mean \pm SEM.

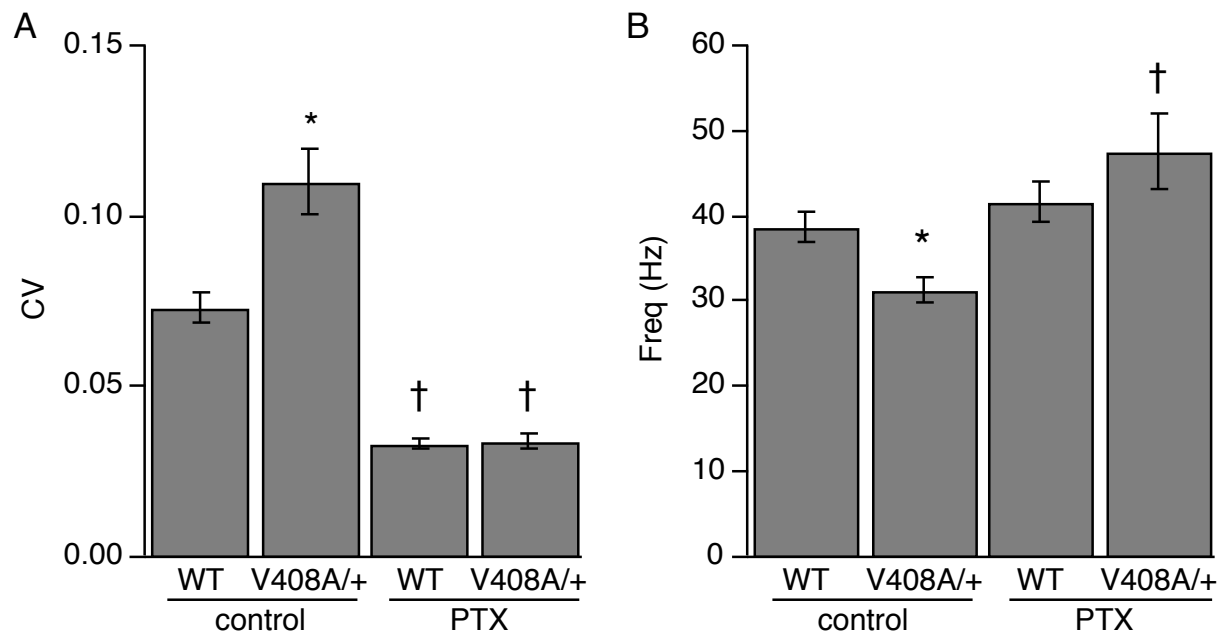


Figure 2.

β -adrenergic modulation of +/V408A firing precision

β -adrenergic receptor activation (BAR) is required to show +/V408A motor deficits, as assessed by accelerating rotarod and balance beam assays (Herson et al., 2003). Thus, the difference in the basal firing properties of Purkinje cells observed in **Fig. 1** is presumably not sufficient to cause a motor deficit. To assess the effects of adrenergic stress on firing precision, we applied the β -adrenergic agonist isoproterenol (ISO, 8 μ M) to brain slices after collecting a control recording (**Fig. 3**). Subsequent PTX application indicated the extent to which ISO effects were mediated through changes in GABAergic signaling. In WT and +/V408A Purkinje cells, ISO increased the CV_{ISI} by $26.9 \pm 5.7\%$ and $50.6 \pm 12.2\%$, respectively (**Fig. 3A**); WT: control = 0.065 ± 0.008 ; ISO = 0.085 ± 0.013 ($n = 16$; $P < 0.001$); +/V408A: control = 0.122 ± 0.02 ; ISO = 0.204 ± 0.047 ($n = 17$; $P < 0.001$). The CV_{ISI} of +/V408A cells was higher than that of WT cells in control conditions ($P < 0.05$), and in ISO ($P < 0.05$). However, the relative increase in CV_{ISI} in response to ISO was not different between the genotypes ($P = 0.22$) (**Fig. 3A**).

PTX reversed the ISO-mediated increase in CV_{ISI} in both genotypes to a level significantly lower than control (**Fig. 3A**); WT: ISO+PTX = 0.036 ± 0.004 ($n = 13$; $P < 0.001$); +/V408A: ISO+PTX = 0.048 ± 0.009 ($n = 11$; $P < 0.001$) indicating that the effects of ISO on CV_{ISI} were exerted through changes in GABAergic

transmission. Indeed, the CV_{ISI} in the presence of ISO+PTX were not different between the two genotypes ($P = 0.62$).

The firing frequency was also analyzed (**Fig. 3B**). In WT Purkinje cells, ISO reduced firing frequency by $27.4 \pm 2.8\%$, from 37.1 ± 3.1 to 27.0 ± 2.5 Hz ($n = 15$, $P < 0.0001$). Subsequent addition of ISO+PTX partially restored the rate to 31.1 ± 2.5 Hz, which differed from ISO ($P < 0.05$), but was still reduced by $17.6 \pm 4.6\%$ from control ($n = 12$, $P < 0.01$). In +V408A Purkinje cells, ISO reduced the firing frequency by $28.4 \pm 3.1\%$, from 33.0 ± 3.2 to 23.9 ± 2.6 Hz ($n = 13$, $P < 0.01$). Subsequent addition of ISO+PTX resulted in a firing frequency of 31.9 ± 2.8 Hz, but this was not a significant increase from ISO alone ($P = 0.3$, $n=7$). This is 96.8% of the firing frequency in control, and the two values did not differ significantly ($P = 0.22$, $n = 7$) (**Fig. 3B**).

Figure 3. β -adrenergic receptor activation reduces action potential firing precision and frequency via GABAergic signaling. *A*, The effect of ISO application on the CV_{ISI} in WT and +V408A Purkinje cells. *B*, Graph of action potential frequency from data in *A*. * indicates difference between condition and control. £ indicates a difference between ISO and ISO+PTX. † indicates difference between genotypes. Data presented as mean \pm SEM. Significance is defined as $P < 0.05$.

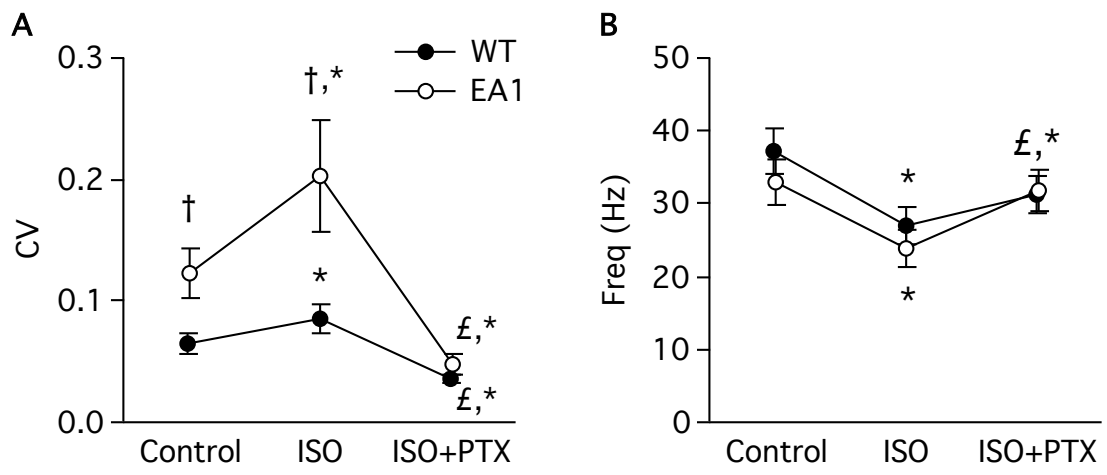


Figure 3.

The effect of β -adrenergic receptor activation on coefficient of variation and frequency is dependent on GABAergic signaling

PTX was shown in **Fig. 3** to reverse the effect of ISO on CV_{ISI} . To confirm that the effects of BAR signaling are strictly via GABAergic signaling, we added PTX first and examined the effect of subsequent addition of ISO. To ensure complete block of GABAARs, we pre-incubated cerebellar slices in PTX for 30 minutes at RT before recording the PTX treated control period at 35 °C (**Fig. 4**). ISO application in the presence of PTX does not significantly change coefficient of variation in either genotype indicating that all or most of the ISO effect is dependent on GABAergic signaling (**Fig. 4A**); WT: PTX = 0.0315; PTX+ISO = 0.0342, n = 12; $P = 0.07$; +/V408A: PTX = 0.0356; PTX+ISO = 0.0432, n = 11; $P = 0.13$. The coefficient of variation did not differ between genotypes in PTX ($P = 0.319$), nor in PTX+ISO ($P = 0.098$). Consistent with the other experiments, the coefficient of variation of PTX treated cells was lower than that of untreated cells shown in **fig. 2** for both WT ($P = 0.002$) and +/V408A ($P = 0.002$). In the presence of PTX, ISO did not change AP frequency in either genotype (**Fig. 4B**; WT: PTX = 46.4Hz; PTX+ISO = 43.0Hz, n = 8; $P = 0.25$; +/V408A: PTX = 45.3Hz; PTX+ISO = 38Hz, n = 8; $P = 0.055$). The frequency did not differ between the genotypes in PTX ($P = 0.90$), or in PTX+ISO ($P = 0.50$). The firing frequency of PTX treated cells did not differ from the frequency of untreated cells shown in **fig. 2** in either WT ($P = 0.12$) or +/V408A ($P = 0.10$) experiments.

Figure 4. The effects of ISO on action potential firing patterns in the absence of GABA_A receptor signaling. *A*, CV_{ISI} for WT and +V408A cells in the presence of PTX followed by PTX+ISO, respectively. *B*, action potential firing frequency for WT and +V408A cells in the presence of PTX followed by PTX+ISO, respectively. Data presented as mean ± SEM.

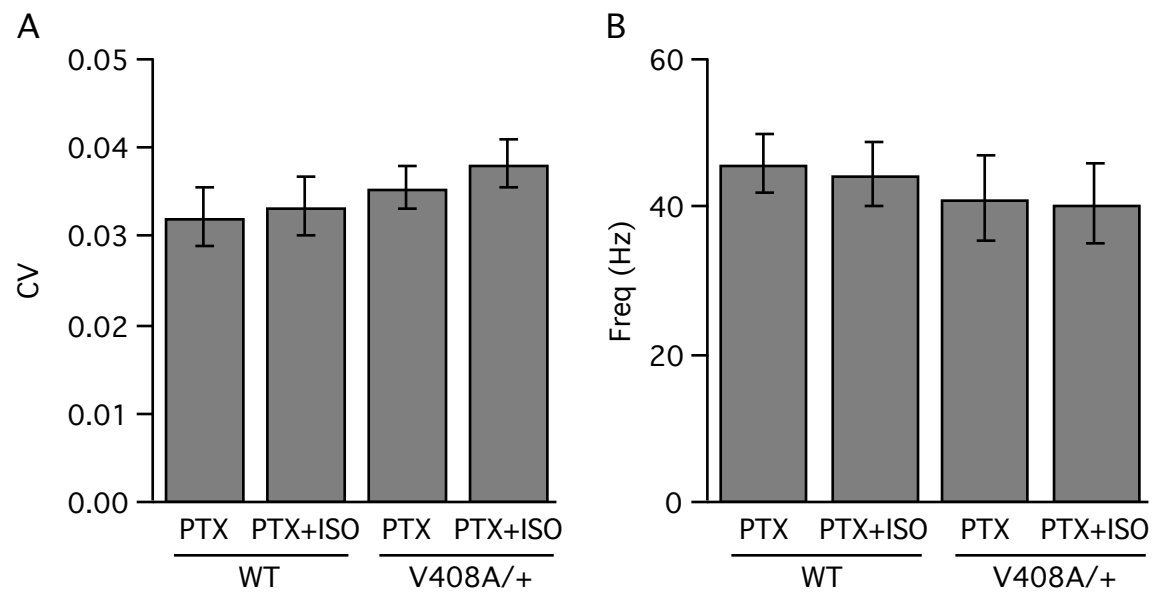


Figure 4.

Acetazolamide ameliorates the +/V408A precision deficit and increases the frequency of firing

We tested the possibility that acetazolamide (ATZ) affects the precision of firing by comparing recordings of ATZ treated (0.5mM) and non-treated cells of each genotype (**Fig. 5A**). Slices were exposed to ATZ for 60 minutes at room temperature before recording, to mimic the strategy employed by +/V408A patients who consume the drug as a prophylactic against attacks. WT and +/V408A control values from **figure 1** are recapitulated here to make comparisons to the +/V408A +ATZ and WT+ATZ data. +/V408A cells in ATZ displayed a lower coefficient of variation than +/V408A control cells (+/V408A control cells = 0.109, n = 53; +/V408A +ATZ = 0.061, n = 24; $P = 0.001$). Interestingly, The average CV_{ISI} of +/V408A +ATZ was not significantly different from WT control cells ($P = 0.07$). ATZ treatment of WT cells did not result in lower CV_{ISI} relative to WT controls (WT= 0.0746, n = 51; WT+ATZ = 0.0576, n = 9; $P = 0.16$).

WT and +/V408A cells treated with ATZ both fire faster than their respective control cells (**Fig. 5B**; WT: control = 39.1Hz, n = 51; WT+ATZ = 55.4Hz, n = 9; $P = 0.0016$; +/V408A = 34.4Hz, n = 53; +/V408A +ATZ = 41.3Hz, n = 26; $P = 0.001$). Interestingly though, ATZ pre-incubated +/V408A cells are not different from WT values ($P = 0.42$).

Figure 5. ATZ occludes the +/V408A effects on action potential precision and frequency. *A*, Bar graph of WT and +/V408A CV_{ISI} in control and in 0.5mM ATZ. Control data are recapitulated from **Fig. 1**. The effects of the +/V408A mutation on CV_{ISI} and action potential frequency are occluded. *B*, Bar graph of action potential frequency. ATZ increased firing rate in both genotypes, relative to untreated cells. Interestingly, the firing rate of +/V408A+ATZ was not different from untreated WT. * indicates differences between control and ATZ treatment within a genotype. † indicates differences between genotypes in the same condition. Significance is defined as $P < 0.05$. Data presented as mean \pm SEM.

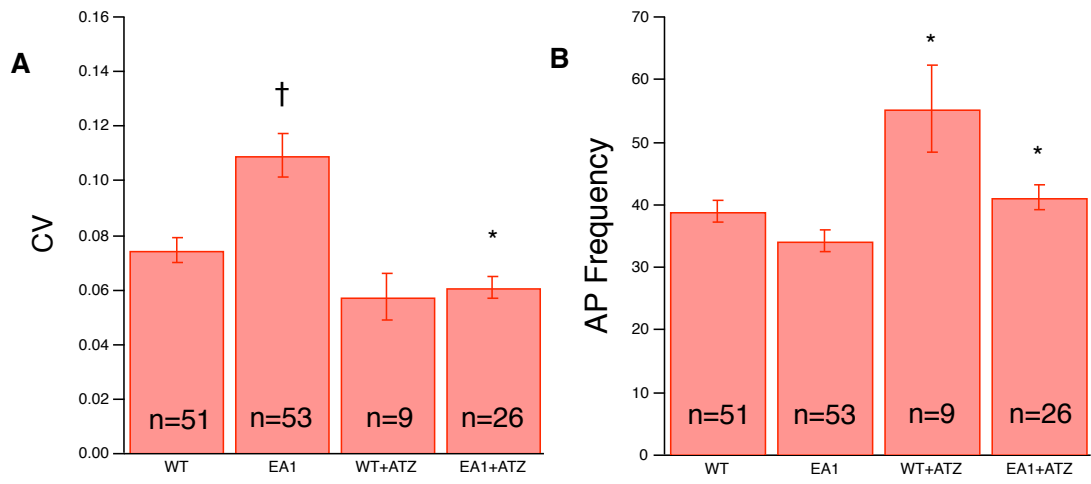


Figure 5.

The effect of β -adrenergic receptor activation is partly occluded in the presence of ATZ

The amelioration of the genotypic precision deficit by ATZ suggests that BAR activation will have less impact on this measure when in the presence of ATZ, as would be the case with an EA1 patient who takes ATZ as a prophylactic before experiencing stress. We tested the effect of ISO on WT and +V408A cells that were previously incubated in 0.5mM ATZ for 30-60 minutes at RT (**Fig. 6**). ATZ was maintained in the bath throughout the subsequent additions of ISO, and of ISO+PTX.

ATZ pre-treated WT cells did not show a significant increase in coefficient of variation in response to ISO (control= 0.0523; ISO= 0.0567, $n = 7$, $P = 0.355$, **Fig. 6A**). Subsequent addition of ISO+PTX reduced the coefficient of variation to 0.036. This was significantly lower than ISO alone ($n = 7$, $P = 0.024$), but not lower than control values in ATZ ($n = 7$, $P = 0.061$). ATZ treatment occluded much of the ISO effect on +V408A cells that was shown in **Fig. 3**. ISO increased the coefficient of variation of +V408A cells in ATZ significantly (control = 0.060; ISO = 0.0763, $n = 14$, $P = 0.0015$, **Fig. 6A**). Subsequent addition of ISO+PTX reduced the coefficient of variation to 0.045, which is lower than control ATZ recordings ($n = 14$, $P = 0.012$) and lower than ISO ($n = 14$, $P = 0.0004$).

Comparison of ATZ+ISO to ISO alone. WT: This increase expressed as a % of the control (13%) did not differ significantly from the increase ISO causes in

WT cells without ATZ (26.9%; $P = 0.2$). Additionally, the CV_{ISL} in ISO in the ATZ group was not different from that of the non-ATZ group ($P = 0.17$). +V408A: While this increase expressed as a % of control (27.8%) is not significantly different from that seen when ISO is added to non-ATZ treated +V408A cells (50.6%), the two resulting values in ISO are different ($P = 0.02$).

Comparison of the control groups: As shown in **figure 1**, +V408A controls have a higher coefficient of variation than WT controls ($P = 0.014$). +V408A + ATZ has a lower coefficient of variation than +V408A ($P = 0.009$), and is not different from WT ($P = 0.57$) or from WT+ATZ ($P = 0.33$). WT+ATZ is not different from WT ($P = 0.35$).

Comparison of the ISO-induced increases in coefficient of variation: As shown in **figure 3**, +V408A +ISO has a higher coefficient of variation than WT+ISO ($P = 0.024$). +V408A +ATZ+ISO has a lower coefficient of variation than +V408A +ISO ($P = 0.02$) (**fig. 6e**), and is not different from WT in ISO ($P = 0.53$), nor is it different from WT+ATZ+ISO ($P = 0.058$). WT+ATZ+ISO was not different from WT+ISO ($P = 0.16$).

Comparison of groups in PTX: As shown in **figure 3**, +V408A and WT cells are not different in ISO+PTX ($P = 0.19$). None of the additional comparisons with ATZ treated cells of either genotype are significantly different in PTX. (+V408A +ATZ+ISO+PTX vs. +V408A +ISO+PTX; $P = 0.73$; and vs. WT+ISO; $P = 0.15$;

and vs. WT+ATZ+ISO+PTX; $P = 0.23$). WT+ATZ+ISO+PTX was not different from WT+ISO+PTX ($P = 0.99$).

ATZ occludes a portion of the ISO effect on frequency of firing (Fig. 6B,C). ISO decreased the firing frequency of +/V408A +ATZ cells from 41.9Hz to 33.2Hz ($n = 14$, $P = 0.0002$) (Fig. 6B). Subsequent addition of ISO+PTX insignificantly increased the frequency to 34.2Hz ($P = 0.14$), which is also still significantly lower than +/V408A +ATZ control recordings ($n = 14$, $P = 0.0003$).

ISO decreased the frequency of WT+ATZ cells from 54.7Hz to 46.7Hz ($n = 7$, $P = 0.021$)(Fig. 6B). Subsequent addition of ISO+PTX insignificantly increased the frequency to 50.2Hz ($P = 0.71$), but this is not significantly lower than WT+ATZ control recordings ($P = 0.27$).

Comparison of the control groups: As shown in **figure 3**, firing frequency in +/V408A controls is not different from WT controls ($P = 0.36$). +/V408A +ATZ has a higher frequency than +/V408A ($P = 0.019$), and is not different from WT ($P = 0.20$), but is slower than WT+ATZ ($P = 0.023$). WT+ATZ exhibits faster firing than WT ($P = 0.012$)(Fig. 6C).

Comparison of the ISO-induced decreases in frequency: As shown in **figure 3**, the frequency of +/V408A +ISO is not different from WT+ISO ($P = 0.39$). +/V408A +ATZ+ISO has a higher frequency than +/V408A +ISO ($P = 0.008$), but is not different from WT in ISO ($P = 0.20$), and is slower than WT+ATZ+ISO ($P = 0.014$). WT+ATZ+ISO fires faster than WT+ISO ($P = 0.002$).

Comparison of groups in PTX: As shown in **figure 3**, the frequency of +/V408A + ISO + PTX is not different from WT+ISO+PTX ($P = 0.83$). +/V408A +ATZ+ISO+PTX is not different from +/V408A +ISO+PTX ($P = 0.50$), or from WT+ISO+PTX ($P = 0.33$), and is slower than WT+ATZ+ISO+PTX ($P = 0.009$). WT+ATZ+ISO+PTX fires faster than WT+ISO+PTX ($P = 0.007$).

We show that the difference in CV_{ISI} between +/V408A +ATZ and +/V408A Ctrl is removed in PTX (**Fig. 6C**), suggesting that the mechanism by which ATZ affects coefficient of variation is dependent on GABAergic signaling, and is redundant with or occluded by- block of GABAARs. To further investigate the action of ATZ in reducing control coefficient of variation in +/V408A cells, and precluding the effects of ISO in both genotypes, we reversed the order of drug application and tested the effects of ATZ in slices that were pre-incubated with PTX. We find that ATZ has no effect on coefficient of variation or frequency of firing in either genotype when GABAergic transmission is blocked. In WT cells, the coefficient of variation of PTX+ATZ/PTX pre-incubated controls = 107% ($P = 0.55$), $n = 3$. Frequency of firing was = 105% ($P = 0.89$). In +/V408A cells, the coefficient of variation of PTX+ATZ/PTX pre-incubated control = 130% ($p = 0.36$), $n = 5$. The firing frequency was 112% ($P = 0.50$).

Figure 6. ATZ occludes the effect of β -AR activation. *A*, Graphs of individual (thin lines) and average (bold) CV_{ISI} in ATZ, ATZ+ISO, and ATZ+ISO+PTX, in WT and +V408A Purkinje cells. *B*, the AP frequency was measured during the experiments described in *A*. *C*, A comparison of the genotypic averages from *A* (left) and *B* (right), now accompanied by graphs from **Fig. 3** showing the effects of ISO in the absence of ATZ. *indicates difference between condition and control within a genotype. £ indicates a difference between ISO and ISO+PTX within a genotype. Significance is defined as $P < 0.05$. Data are presented as mean \pm SEM.

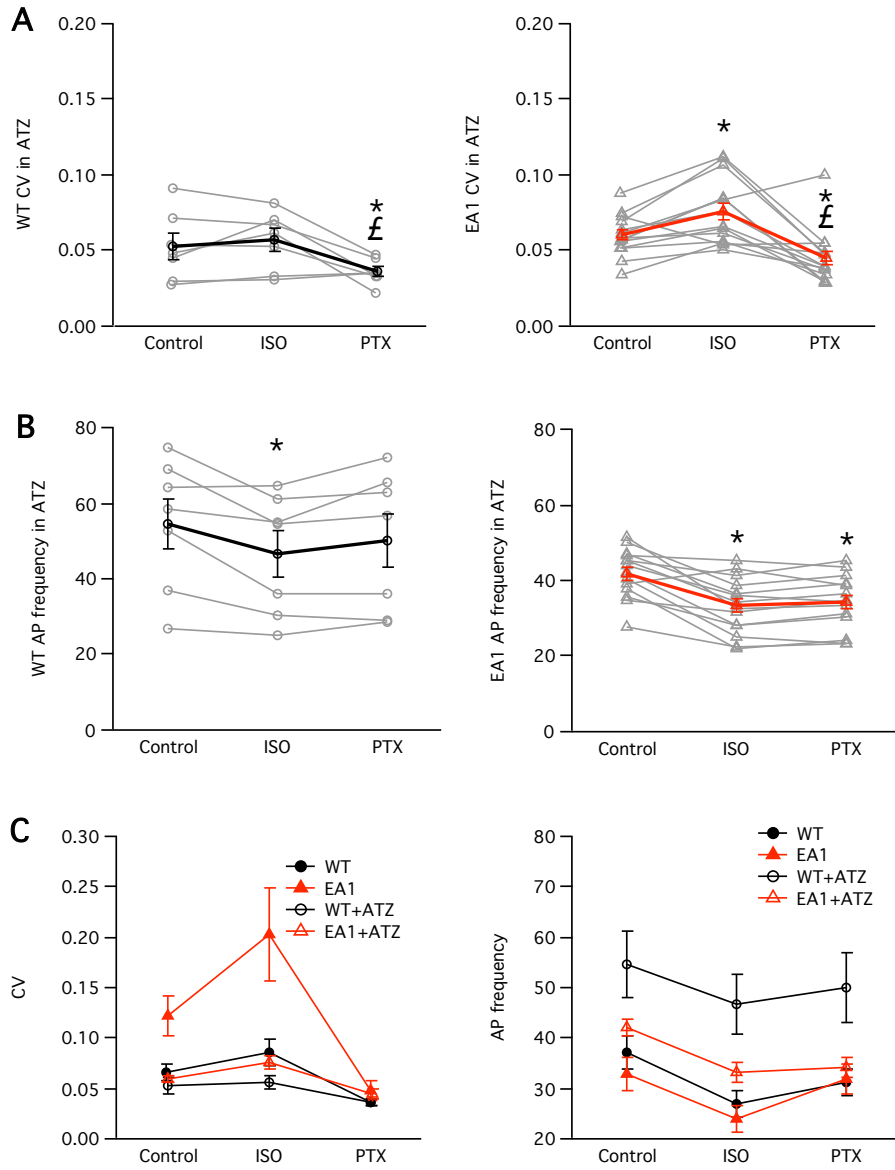


Figure 6.

Discussion

We studied a +/V408A mouse model of EA1, which receives excessive GABAergic input to Purkinje cells. Our results indicate that increased inhibitory tone reduced firing precision as well as firing frequency. This precision deficit was exacerbated by β AR activation. Acetazolamide ameliorated the +/V408A precision deficit and occluded the effect of β AR activation on Purkinje cell pacemaking. These results are consistent with the hypothesis that a reduced precision +/V408A phenotype, exacerbated by β AR activation during stress, underlies motor deficits in EA1, and that acetazolamide ameliorates EA1 motor deficits by restoring the precision of the interval during β AR activation.

Pacemaking precision in Purkinje cells

Purkinje cell firing encodes the summation of all cerebellar processing to form the sole output from the cerebellar cortex. The spontaneous regular firing of Purkinje cells allows for bi-directional modification by excitatory and inhibitory contacts (Eccles, 1973). Information from Purkinje cells is conveyed not only through the constant rate of tonic firing but also, and perhaps more importantly, through rate and mode changes. +/V408A Purkinje cells fired action potentials with a higher CV_{ISI} than WT. The level of precision of the inter-spike interval is critical for resolving rate changes. This is dramatically illustrated in mice harboring

mutations in P/Q-type Ca_v channels that approximate EA2 (Hoebeek et al., 2005; Walter et al., 2006). In the P/Q-type Ca_v channel mutation *ducky*, deficits in intrinsic firing precision obscure the Purkinje cell response to incoming parallel fiber signaling, and appear to have a causal role in abnormal behavioral phenotypes (Walter et al., 2006).

GABAergic tone and firing precision of Purkinje cells

Blocking GABAergic transmission onto WT Purkinje cells reduces the CV_{ISI} , indicating that basal GABAergic signaling contributes to imprecision of the interspike interval (Hausser and Clark, 1997). The V408A mutation increases GABAergic signaling from basket cells onto Purkinje cells (Herson et al., 2003). In our experiments, the elevated CV_{ISI} in +/V408A Purkinje cells resulted from increased GABAergic input, and blocking GABA_A receptors completely equalizes the CV_{ISI} between EA1 and WT Purkinje cells (**Fig. 2**), demonstrating its causality in this difference. Blocking GABAergic input with PTX increases Purkinje cell firing frequency in WT (Hausser and Clark, 1997a). In agreement with this observation, +/V408A Purkinje cells displayed reduced firing frequency compared to WT controls. Blocking GABA_A receptors in WT Purkinje cells did not significantly affect firing frequency. In contrast, blocking GABA_A receptors in +/V408A Purkinje cells increased the average firing rate compared to untreated +/V408A Purkinje cells. This genotype-specific effect of PTX on firing frequency,

affecting +/V408A but not WT Purkinje cells, is consistent with the increased GABAergic tone of the mutant Purkinje cells. The central role of GABAergic tone is further evidenced by the finding that the two genotypes do not differ in either CV_{ISI} or frequency of firing when GABAergic transmission is blocked. Indeed, the genotypic difference is only revealed when GABAergic transmission is left intact, consistent with the hypothesis that the increased GABAergic input in +/V408A Purkinje cells is sufficient to alter their firing activity. However, this basal increase of GABAergic tone in EA1 Purkinje cells is apparently not sufficient to cause a motor deficit as our previous studies showed that stress (e.g. β -adrenergic receptor activation) is additionally required to reveal motor-deficits in +/V408A mice (Herson et al., 2003).

Why is the ataxia in EA1 episodic?

Adrenergic signaling is associated with stress, which can induce attacks of EA1 in human patients. Noradrenaline, acting through presynaptic β 2-adrenoceptors, elicits long-term facilitation of GABAergic transmission from Basket cells onto Purkinje cells, resulting in increased inhibitory postsynaptic currents (IPSCs) in Purkinje cells (Llano and Gerschenfeld, 1993, (Saitow et al., 2000). This increased inhibitory tone depresses the output of the cerebellar cortex (Mitoma and Konishi, 1996, 1999), suggesting that increased GABAergic transmission in response to stress may augment the increased inhibition caused by the V408A

mutation, resulting in a larger decrease in Purkinje cell firing regularity and consequent motor dysfunction. In basket cells, β -adrenergic receptor activation (β -AR) increases cAMP that binds directly to HCN-1 channels and shifts their activation voltage to more positive potentials, making smaller hyperpolarizations sufficient to activate the channels. This results in a more excitable presynaptic terminal and increased GABA release (Saitow and Konishi, 2000). Application of the β -AR agonist, isoproterenol increases the CV_{ISI} of both WT and +/V408A Purkinje cells. The CV_{ISI} of +/V408A cells was significantly higher than that of WT cells in control conditions, and in ISO. However, the increase in CV_{ISI} as a percentage of control was not different between the genotypes, indicating that ISO acts similarly in both genotypes. Therefore, it is likely that increased GABAergic transmission in response to stress summates with the increased inhibition caused by the V408A mutation to elevate the Purkinje cell CV_{ISI} above a threshold for cerebellar dysfunction. PTX reversed the ISO-mediated increase in CV_{ISI} in both genotypes to a level significantly lower than control, confirming that the effects of ISO were exerted through increases in GABAergic transmission. Indeed, the CV_{ISI} of the two genotypes in ISO+PTX was not different. The firing frequency of +/V408A Purkinje cells did not differ from WT Purkinje cells in control, ISO, or PTX conditions. If Purkinje cell firing frequency was related to EA1 attacks, you would expect this measure to be different between WT and +/V408A Purkinje cells during the stress paradigm. Because

the frequency of firing in ISO does not differ between genotypes (whereas the CV_{ISI} does), it is unlikely that the ISO effect on frequency causes the ataxic phenotype.

ISO reduced firing frequency in both genotypes, and subsequent addition of PTX ameliorated frequency in both genotypes. But while it was restored completely in +/V408A Purkinje cells, the reversal was not completed in WT. To assess whether ISO was having an effect in WT cells that was independent of GABA, we blocked $GABA_A$ receptors first using PTX, followed by addition of ISO. With GABAergic transmission blocked, the addition of ISO showed no change in CV_{ISI} in either genotype. This confirms that the effects of BAR signaling are via GABAergic signaling. The coefficient of variation did not differ between genotypes in PTX, nor in PTX+ISO. In the presence of PTX, ISO did not change AP frequency in either genotype. The frequency did not differ between the genotypes in PTX, or in PTX+ISO.

ATZ ameliorates the +/V408A precision deficit and occludes the majority of the effect of β -AR activation

The carbonic anhydrase inhibitor ATZ reduces the frequency and severity of attacks in many EA1 patients, but its mechanism of action is not known. Here, we show that ATZ reduces CV_{ISI} in +/V408A cells to levels not different from WT. This supports the hypothesis that the imprecision of +/V408A Purkinje cell firing

underlies the motor deficit. The amelioration of the precision deficit by ATZ suggests that β -AR activation will have less impact on this measure in the presence of ATZ, as would be the case with an EA1 patient who takes ATZ as a prophylactic before experiencing stress. Indeed, ISO fails to increase the CV_{ISI} of WT cells when they are pre-treated with ATZ, and +/V408A cells treated with ATZ displayed an increased CV_{ISI} in response to ISO, but this was still significantly lower than +/V408A cells in ISO without ATZ.

Chapter III

Reduced expression of SK2 alters intrinsic Purkinje cell firing and motor coordination

ABSTRACT

The regularity of Purkinje cell pacemaking is thought to be critical to cerebellar function and cerebellar-dependent motor control. Pharmacological block of the small conductance calcium-activated potassium channel SK2 alters the frequency and pattern of Purkinje cell action potentials. We find that reduced SK2 expression causes aberrations of Purkinje cell firing patterns in most cerebellar lobules, I-VIII and X. Regular tonic firing was retained in lobules VIII and IX, suggesting that regularity of Purkinje cell firing in this region is SK2-independent. Despite the irregularity of Purkinje cell firing in most lobules, these animals showed no motor deficit on either the accelerating rotarod or the balance beam. We surgically ablated lobules VIII and IX. This ablation rendered the vermis devoid of regular firing Purkinje cells in SK2^{fl/fl} mice, while leaving a majority of the regularly firing Purkinje cells of the WT vermis intact. These ablations reveal a motor deficit in SK2^{fl/fl} mice in the balance beam assay, but had no effect in WT mice. This supports the notion that regular tonic Purkinje cell firing is important for cerebellar-dependent motor coordination. Conversely, lobule VIII and IX ablation SK2^{fl/fl} animals show no deficit on the accelerating rotarod. This indicates that the abilities challenged by this assay are not dependent on Purkinje cell pacemaking in the vermis.

INTRODUCTION

The cerebellum is involved in posture, balance, motor planning and movement execution (Ito, 1984). Various ataxias result from mutations that affect cerebellar processing (Manto and Pandolfo, 2002; Manto and Marmolino, 2009). Purkinje cells are an example of pacemaker neurons, which fire spontaneously with regular intervals, and are the sole output of the cerebellar cortex (Hausser and Clark, 1997a; Raman and Bean, 1999).

The SK-specific channel blocker apamin increases Purkinje cell firing frequency, and converts tonic Purkinje cell firing into bursting patterns (Womack and Khodakhah, 2003). Of the three mammalian SK subunits expressed in central neurons, only SK2 is expressed in Purkinje cells (Cingolani et al., 2002; Womack and Khodakhah, 2003). Both somatic and dendritic SK2 channels contribute to control of action potential firing in Purkinje cells.

Regularity of Purkinje cell firing has been shown to underlie cerebellar-dependent motor control (Hoebeek et al., 2005). This result implies that aberrant or reduced SK2 channel activity may negatively impact motor coordination. Indeed, reduced Purkinje cell SK2 activation has been reported to underlie the motor deficits of animal models of episodic ataxia type 2 (EA2) (Walter et al., 2006). EA2 is linked to mutations in P/Q-type voltage-gated calcium channels (VGCC) or their auxiliary subunits (Pietrobon, 2002). These mutants, *ducky* and *leaner*, exhibit deficits in Purkinje cell firing regularity and motor coordination, as

assayed by the accelerating rotarod and balance beam. VGCC-related mutations directly decrease calcium influx, reducing SK2 activation, and resulting in irregular Purkinje cell firing and deficits in rotarod performance. EBIO, which increases SK2 activation by increasing the apparent calcium sensitivity of SK channels, restores Purkinje cell firing precision in *leaner* and *ducky* mice, and ameliorates motor deficits in *ducky* and *tottering* mice (Walter et al., 2006). An alternate SK activator, chlorzoxazone, also restores *tottering* Purkinje cell firing regularity *in vitro* and motor performance *in vivo* (Alvina and Khodakhah, 2010).

If reduced activation of SK2 causes EA2, reduced expression of SK2 would be expected to phenocopy the disease. We have used a genetic mouse model of reduced SK2 expression, homozygous floxed SK2 mice (SK2^{fl/fl}) (Bond et al., 2004), to investigate the involvement of SK2 channels in regulating Purkinje cell firing patterns, and the necessity of regular firing for ability in motor control assays. We studied intrinsic Purkinje cell pacemaking in acute cerebellar slices with fast synaptic transmission blocked. SK2^{fl/fl} mice display regular Purkinje cell pacemaking in only 2 lobules (VIII and IX) of the cerebellum, and yet show no overt motor deficit. Ablation of lobules VIII and IX in SK2^{fl/fl} mice reduces their ability on the balance beam, and has no effect on WT animals, supporting the notion that Purkinje cell pacemaking is required for cerebellar-dependent motor tasks. Conversely, ablations did not impact SK2^{fl/fl} ability on the accelerating

rotarod. These results suggest that the two motor control assays have differing dependence on Purkinje cell pacemaking.

METHODS

Slice preparation. 300µm sagittal cerebellar slices were obtained from the vermis of WT or SK2^{fl/fl} mice (4-12 weeks old). Mice were deeply anesthetized with a cocktail of ketamine (30mg/8.5ml) and xylazine (2.9mg/8.5ml) at 0.1cc/25g bodyweight. Mice were then perfused through the left ventricle with 30ml of ice-cold ACSF (pH 7.4) before the brain was removed and the cerebellum dissected. Ice-cold ACSF was used to bathe the tissue during dissection. The ACSF was bubbled continuously with 5%CO₂/95%O₂. Sagittal sections of the vermis were taken on a Leica VT-1000s. Sections were incubated at 35 °C for 30 minutes, and then kept at room temperature until used for recordings. Slices were transferred one at a time to the recording chamber, which was continuously perfused with oxygenated ACSF containing 40µM DNQX to block AMPA and Kainate sensitive glutamate receptors, 80 µM picrotoxin to block GABA_A receptors, and 1µM CGP55845 hydrochloride to block GABA_B receptors. Recording ACSF additionally contained 100nM apamin or 5µM NS309 for some experiments. The temperature of the bath was elevated to 35°C just prior to- and for the duration of the recordings. All slices were used within 5 hours of sectioning.

Electrophysiology and analysis. Extracellular current clamp recordings were taken from the axon hillock region of Purkinje cell somas (identified by morphology and location), and visualized with infrared DIC (controlled by a Hamamatsu C2400 camera) on a Leica DMLFS upright microscope. Recordings were made in Patchmaster using an EPC 10 double patch clamp amplifier (Heka Instruments Inc, Bellmore NY) interfaced to a Macintosh G4 computer (Apple, Cupertino, California) with a built in ITC-18, and analyzed using macros written in Igor (Wavemetrics, Portland, OR). Data were collected at a sample frequency of 10 kHz and filtered at 3kHz. Recording pipettes (1.5-2.5 M Ω) contained ACSF.

All data are reported as mean \pm SEM, except where noted to be \pm SD. Comparisons were made by paired and unpaired t-tests as appropriate. Results were considered to be statistically significant when $P < 0.05$, or lower where noted. All significant results are designated.

Solutions. ACSF solution was composed of 119 mM NaCl, 2.5 mM KCl, 1.3 mM MgCl₂-6H₂O, 1 mM Na₂HPO₄, 26.2 mM NaHCO₃, 10 mM glucose, and 2.5 mM CaCl₂-2H₂O.

Accelerating rotarod. Mice were trained on an accelerating rotarod (20 rev/min², 6-cm diameter), with a non-slip surface (Economex by Columbus Instruments, Columbus, Ohio). Training parameters were based on previous experiments

(Rustay et al., 2003). Mice ran 8 consecutive trials, first on the practice day, then on three consecutive test days. Mice were given a minimum of 30 seconds to rest between trials.

Balance beam. The balance beam was custom built from plastic. Dimensions measure 90cm long and 1.5cm wide with a flat surface, and it was suspended 40cm above bedding. On the day before testing, mice were trained to walk the length of the beam using food as a lure. Preliminary experiments determined that four successive trials were sufficient to show minimal foot slips the following day, and for the mice to cross the beam without additional prodding. Test trials were video recorded, and the number of hindfoot missteps was tallied.

Ablation surgery. Eighteen mice (8 WT and 10 SK2^{fl/fl}) were anesthetized with ketamine hydrochloride (60 mg/kg), xylazine (4 mg/kg). Mice were fixed into a restraint apparatus consisting of an incisor bar and an adjustable pin in each ear canal. The occipital bone overlying overlying folia VIII and IX was exposed and removed. The atlanto-occipital membrane was opened and a suction pipette was applied to aspirate lobules VIII and IX. Antibacterial gel foam was inserted to fill the void. The occipital bone was flipped back up into place, and the muscles and skin were sutured up in layers over it. Animals were given 48 hours to recover before behavioral testing. No infections were observed during recovery,

behavioral testing, or post-mortem analysis. Mice were housed and handled in accordance with IACUC and National Institutes of Health experimental guidelines.

Results

SK2^{fl/fl} Purkinje cells show decreased pacemaking precision and increased firing frequency

We previously reported that SK2 expression in whole-brain homogenates is reduced to 20% of WT. Western blots performed on proteins prepared from cerebellar vermis from WT and SK2^{fl/fl} mice (14-17 weeks old) showed that SK2 expression is also specifically reduced in the vermis (**fig. 1**). We examined Purkinje cell firing precision in acute cerebellar slices from SK2^{fl/fl} and WT vermis (**fig. 2** and **fig. 3**). Extracellular recordings of action potentials were made in current clamp. The frequency of action potentials and the coefficient of variation of the inter-spike intervals were calculated.

We limited our survey to lobules I through VII. The results show a dramatic impairment of firing precision in SK2^{fl/fl} Purkinje cells. Autocorrelation of the inter-spike intervals from WT recordings show discrete peaks indicating highly uniform intervals between action potentials (**fig. 2a**). A WT sample trace of Purkinje cell action potentials shows regular inter-spike intervals (**fig. 2a**, inset). In contrast, autocorrelation of a sample recording from SK2^{fl/fl} Purkinje cells shows much reduced regularity of the inter-spike interval (**fig. 2b**). A sample trace of action potentials from the same cell shows visibly irregular inter-spike intervals (**fig. 2b**, inset).

Figure 1. SK2 protein is greatly reduced in the vermis of SK2^{fl/fl} cerebellum. A western blot from vermis-specific homogenates of WT and SK2^{fl/fl} cerebellum.

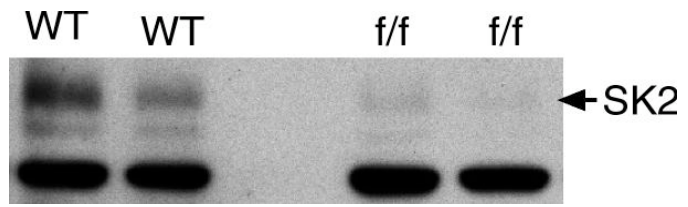


Figure 1

Figure 2. Precision of pacemaking is greatly reduced in SK2^{fl/fl} cerebellum. Sample autocorrelations of inter-spike intervals from extracellular action potential recordings (insets) of WT (left) and SK2^{fl/fl} (right) Purkinje cells from lobule V.

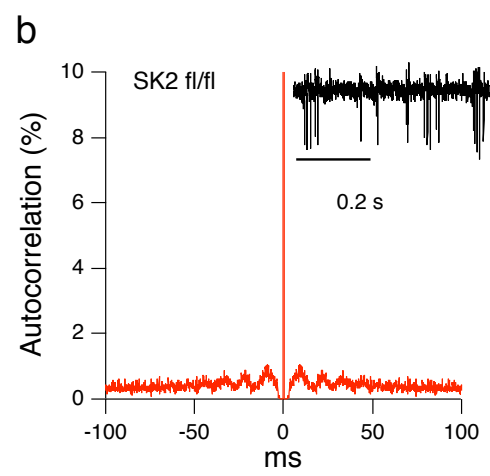
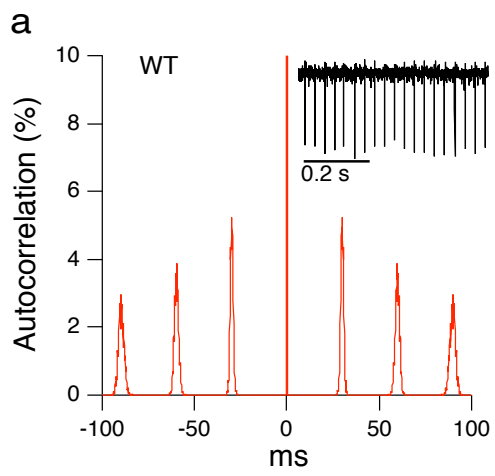


Figure 2.

The CV observed in SK2^{fl/fl} Purkinje cells was higher than in WT cells (WT CV=0.074 ± 0.005, n=51; SK2^{fl/fl} CV=0.432 ± 0.099, n=13, $P < 0.001$) (**fig. 3a**). SK2^{fl/fl} Purkinje cells also fire at a higher frequency than wt Purkinje cells (wt = 39.1Hz ± 1.7, n=51, SK2^{fl/fl} = 141.2Hz ± 23.6, n= 13, $P < 0.001$) (**fig. 3b**).

SK2^{fl/fl} firing behavior does not respond to pharmacological manipulation of SK2

Knock-down of SK2 is incomplete in the SK2^{fl/fl} mouse. We tested the possibility that a reduced amount of SK2 continues to make a contribution to pacemaking in SK2^{fl/fl} Purkinje cells by applying apamin and NS309. NS309 increases the apparent Ca²⁺ sensitivity of SK2 channels. If residual SK2 is contributing to pacemaking in the SK2^{fl/fl} Purkinje cells, NS309 might ameliorate the precision deficit and/or the high firing frequency phenotype. Similarly, the specific SK channel blocker apamin might either exacerbate these phenotypes, or occlude the NS309 effect. After the control recordings, we applied NS309 (5μM) to 8 of the SK2^{fl/fl} cells reported above (**fig. 3**). NS309 did not affect the pacemaking deficit or significantly alter the frequency of firing relative to SK2^{fl/fl} control recordings (NS309 CV = 0.440 ± 0.10, n=8, *P* = 0.115; NS309 frequency = 73.5Hz ± 8.6, n=8, *P* = 0.109) (**fig. 3a,b**). Similarly, application of apamin (100nM) to all 13 SK2^{fl/fl} Purkinje cells did not affect the pacemaking deficit or significantly alter the frequency of firing relative to SK2^{fl/fl} control recordings (apamin CV = 0.474 ± 0.10, n=13, *P* = 0.118; Apamin frequency = 125.1Hz ± 23.3, *P* = 0.981) (**fig. 3a,b**), nor were CV or frequency in apamin different from the preceding NS309 treatment for CV (*p*=0.597) (*P* = 0.103). Finally, the application of NS309 to SK2^{fl/fl} Purkinje cells did not reverse the precision deficit when compared to WT controls (*P* < 0.001), and the difference in firing frequency

was also maintained ($P < 0.001$). We additionally performed preliminary experiments testing the effects apamin on the regularity of WT Purkinje cell interspike intervals. Each experiment showed a clear increase in both CV and frequency. The average CV in control was 0.089 ± 0.028 , and this was increased to 0.467 ± 0.363 in apamin ($n=2$) (**fig. 3a**). The average frequency in control was $49.7\text{Hz} \pm 12.0\text{Hz}$, and this was increased to $96.1\text{Hz} \pm 59.75\text{Hz}$ in apamin ($n=2$) (**fig. 3b**). The average CV and frequency values in WT+apamin recordings were similar to those from . Together with the lack of NS309 amelioration or apamin exacerbation in the $\text{SK2}^{\text{fl/fl}}$ experiments described above, this indicates that SK2 makes no contribution to regulation of firing patterns in $\text{SK2}^{\text{fl/fl}}$ Purkinje cells, despite the knock-down being incomplete.

Figure 3. SK2^{fl/fl} action potentials are faster and less regular than WT, to a degree that is consistent with total knock down of SK2, and do not respond to pharmacological manipulation of SK2. a) The CV was compared between wt cells and SK2^{fl/fl} cells. SK2^{fl/fl} cells were then treated with NS309 and/or apamin. * indicates a difference from WT control ($P < 0.001$). b) Same as in (a), but regarding action potential frequency.

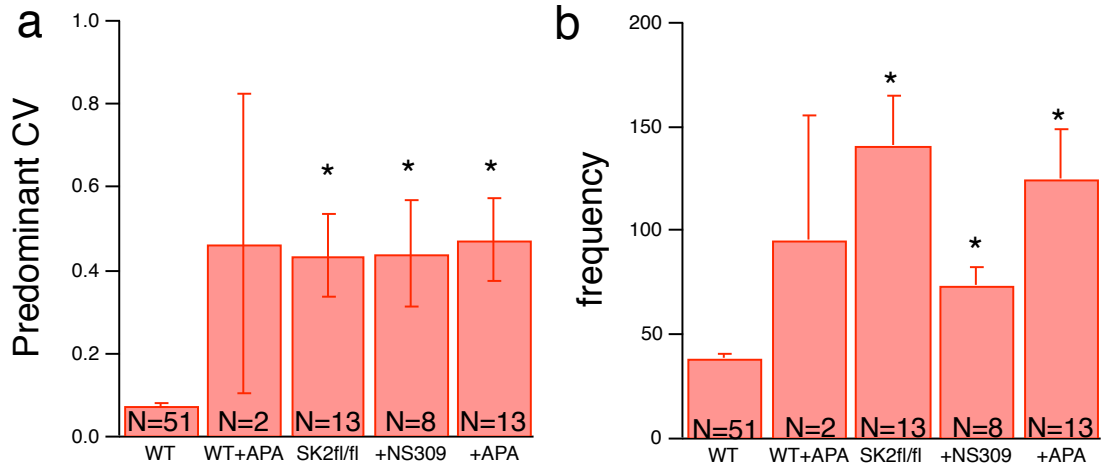


Figure 3.

SK2^{fl/fl} animals do not display a motor deficit

The reduced precision of firing and increased overall frequency seen in the SK2^{fl/fl} Purkinje cells suggested that the SK2^{fl/fl} mice might have motor coordination deficits. Therefore, we tested WT and SK2^{fl/fl} mice in two assays thought to be relevant to cerebellar dysfunction: the accelerating rotarod and the balance beam. Initial comparisons of SK2^{fl/fl} mice and their WT littermates showed no significant difference in their ability to perform and acquire the accelerating rotarod task over eight successive trials for 3 consecutive days (**fig. 4a-c**). Latency-to-fall was recorded and scores were averaged for each trial; each trial average was compared between genotypes by repeated measures ANOVA. The performance score (average of all trials in a day) of SK2^{fl/fl} animals was higher than WT on day 2 (SK2^{fl/fl} = 36.7s; WT = 32.0s. $P = 0.02$, not indicated on graph) (**fig. 4b**). Although the performance score is a less conservative index than repeated measures ANOVA, the result serves to underscore the absence of a deficit in SK2^{fl/fl} mice. Similarly, SK2^{fl/fl} mice and their WT littermates were equally proficient at walking across the balance beam, with the same number of hindfoot missteps: 1.6 ± 0.27 ($n = 16$), and 1.6 ± 0.33 ($n=16$), respectively (**fig. 4d**). These results show that SK2^{fl/fl} and WT mice are equally proficient on the accelerating rotarod and balance beam.

Figure 4. SK2^{fl/fl} animals do not display a motor deficit. (a-c) Latency to fall from the accelerating rotarod during eight successive trials on 3 consecutive days (WT, circles, n = 16; SK2^{fl/fl}, triangles, n = 16). Genotypes were compared by repeated measures ANOVA for each trial, and showed no significant differences. (d) Hindfoot missteps were counted while each mouse traversed the balance beam, and scores were compared by t-test.

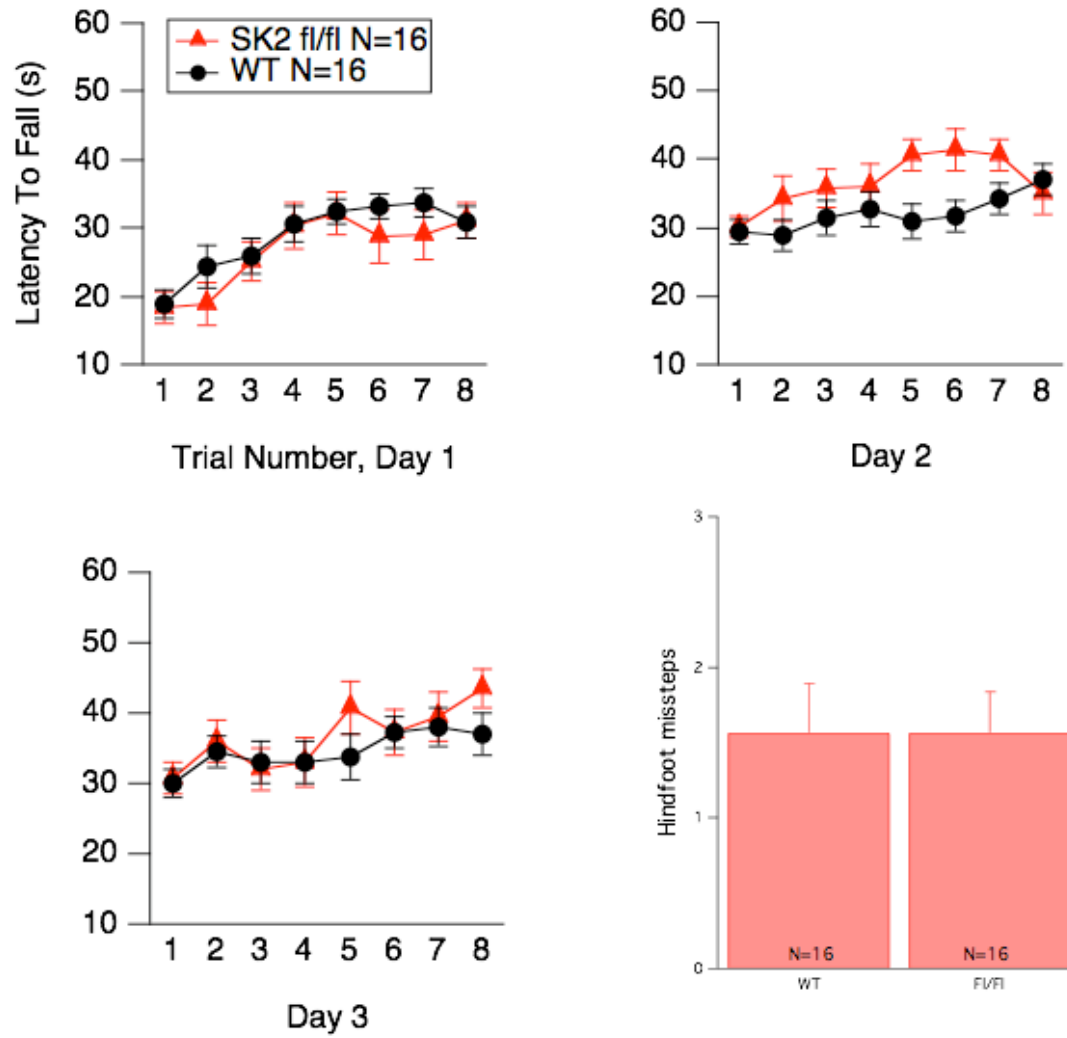


Figure 4.

Lobule-specific Purkinje cell firing behavior in the SK2^{fl/fl} cerebellum

The regularity of Purkinje cell firing is thought to be important for motor coordination. SK2^{fl/fl} animals have irregular Purkinje cell firing in lobules I-VII but lack a motor deficit. Thus we wondered whether regular firing existed in lobules VIII-X, which could maintain motor ability. When these regions were assessed, the results showed that SK2^{fl/fl} Purkinje cells exhibit regular pacemaking in a region that includes parts of lobules VIII and IX (**fig. 5**). Autocorrelation of the inter-spike intervals from a SK2^{fl/fl} cell in lobule VIII shows discrete peaks reflecting highly uniform intervals between action potentials (**fig. 5b**), and the voltage trace shows uniform inter-spike intervals (**fig. 5b**, inset). The average SK2^{fl/fl} lobule VIII CV = 0.031 ± 0.005 , which was lower than that for lobules I-VII ($P < 0.001$, $n = 16$), and was as precise as in WT (**fig. 5c**). Similarly, the frequency = $43.7 \pm 3.1\text{Hz}$, which was lower than I-VII ($P < 0.001$), was not different from WT (**fig. 5d**).

Figure 5. Purkinje cells in lobules VIII and IX of the SK2^{fl/fl} cerebellum display pacemaking. (a) Anatomy and nomenclature of the cerebellar lobules. (b) An autocorrelelogram of inter-spike intervals from a sample recording of SK2^{fl/fl} Purkinje cell action potentials from lobule VIII, with a sample voltage trace (inset). (c) The average CV in SK2^{fl/fl} Purkinje cells from lobule VIII is lower than in lobules I-VII, and not different from WT. (d) firing frequency in SK2^{fl/fl} cells from lobule VIII is lower than in lobules I-VII, and not different from WT. (c and d) SK2^{fl/fl} lobule I-VII n = 13, SK2^{fl/fl} lobule VIII-IX n = 16, WT lobule I-VII n = 51. ** $P < 0.001$.

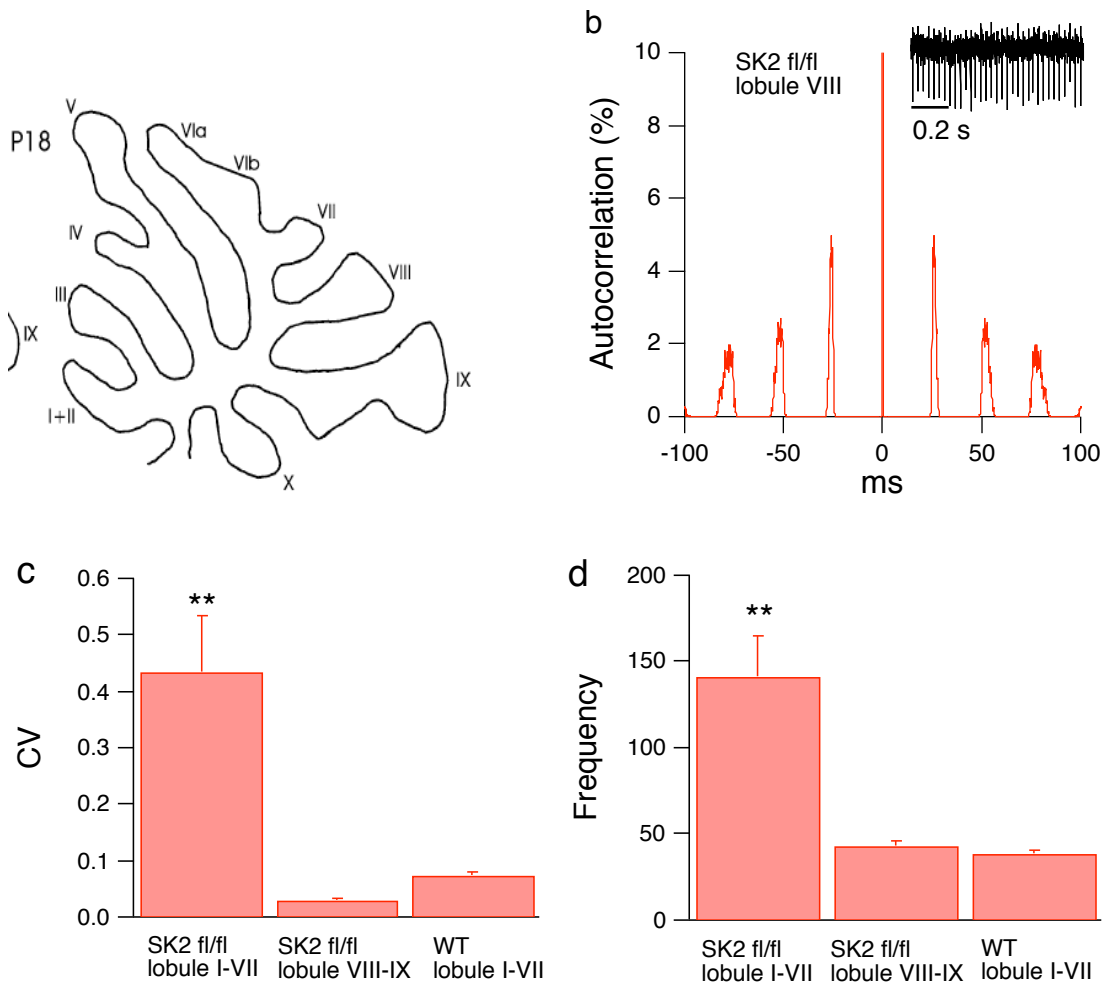


Figure 5.

Ablation of lobules VIII and IX reveals a motor deficit in SK2^{fl/fl} mice

A complete survey of SK2^{fl/fl} vermis reveals Purkinje cell precision of pacemaking equal to WT only in lobules VIII and IX, and yet these mice do not display motor deficits. These results suggest three possibilities: 1. Lobules VIII and IX are sufficient to maintain coordination at the resolution provided by the two behavioral assays; 2. Folia VIII and IX comprise the only important region for these motor coordination tests; 3. Regularity of Purkinje cell pacemaking is not necessary for this kind of motor coordination. To distinguish between these possibilities the grey matter from lobules VIII and IX was surgically ablated in WT and SK2^{fl/fl} mice and the animals were re-tested for balance beam and accelerating rotarod performance (**fig. 6 and fig. 7**). Animals were given 48 hours to recover from surgery, before performing behavioral assays.

Ablation resulted in increased hindfoot missteps in SK2^{fl/fl} animals relative to fl/fl sham surgery controls (fl/fl-ablate = 4.86 ± 0.74 , n = 7; fl/fl-sham = 0.33 ± 0.33 , n = 3, * $P < 0.01$) (**fig. 6**). Ablations in WT mice did not significantly increase their hindfoot missteps relative to WT sham surgery controls (WT-ablate = 1.6 ± 0.51 , n = 5; WT-sham = 0.33 ± 0.33 , n = 3). The four surgery cohorts as well as the two original genotypic cohorts (from fig. 5) were inter-compared. The number of hindfoot missteps in the SK2^{fl/fl} ablation group was significantly higher than each

of the other five groups ($P < 0.05$), and no other comparisons were significantly different.

Figure 6. Ablation of lobules VIII and IX causes a motor deficit only in SK2^{fl/fl} animals. Animals received either sham or ablation surgery. Following a 48-hour recovery period, hindfoot missteps were counted while mice traversed the balance beam. The right panel is re-scaled and repeated from fig. 4, and is included in the comparisons. * $P < 0.05$.

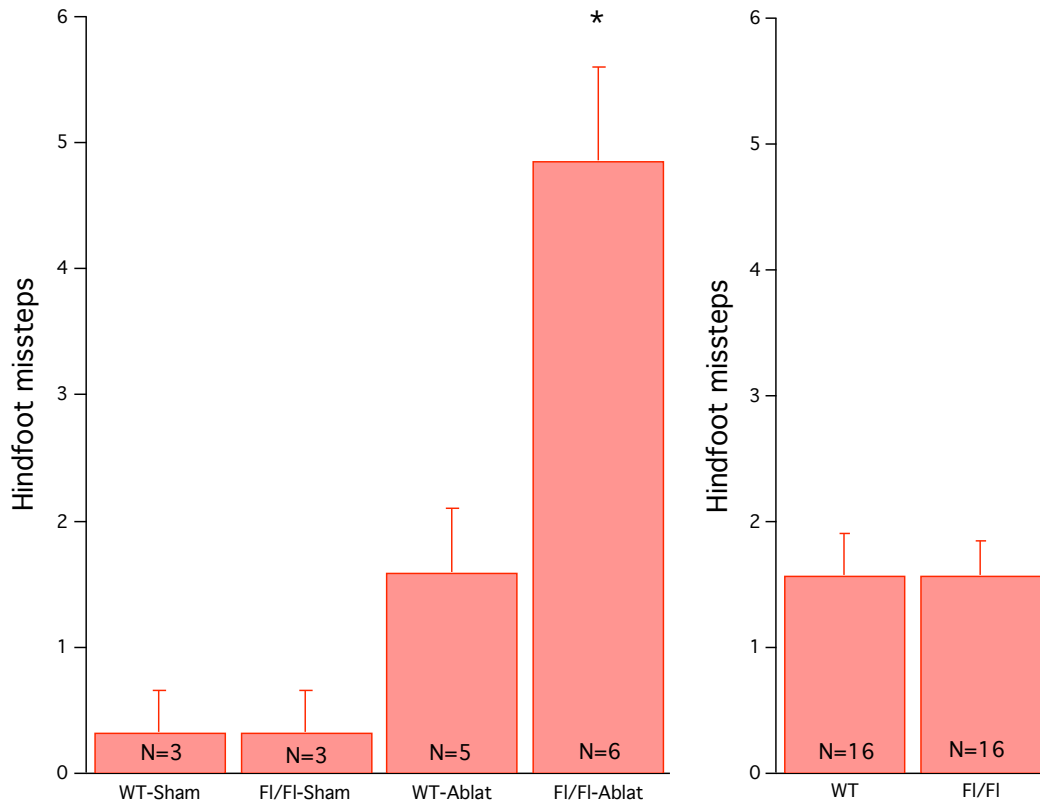


Figure 6.

Figure 7. Ablation of pacemaking region in SK2^{fl/fl} cerebellum does not reduce rotarod ability relative to either sham surgery or genotype. Latency to fall from the accelerating rotarod during eleven successive trials (WT sham, filled circles, n = 3; SK2^{fl/fl} sham, filled triangles, n = 3; WT ablation, empty circles, n = 5; SK2^{fl/fl} ablation, empty triangles, n = 7), both 48 and 72 hours post surgery. Trials were compared by repeated measures ANOVA.

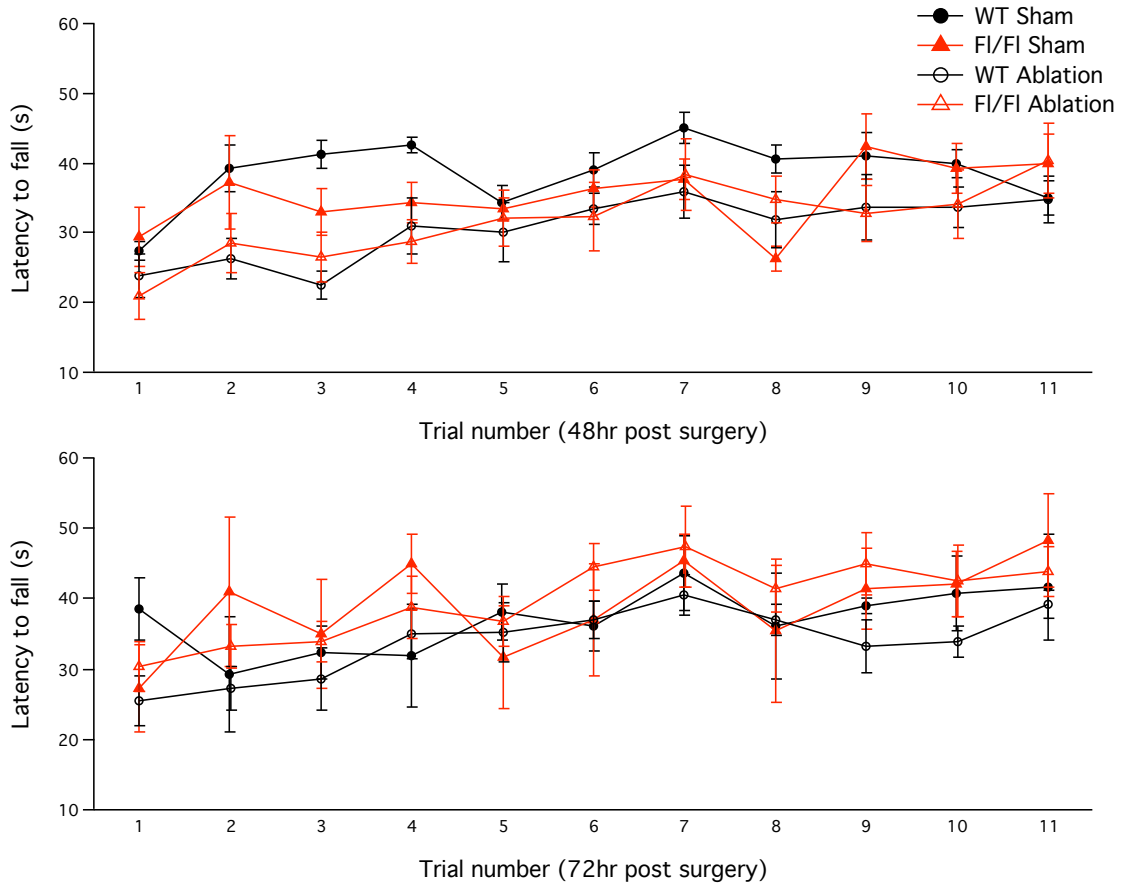


Figure 7.

DISCUSSION

SK2 knock down causes Pacemaking deficits

Of the three mammalian small conductance Ca⁺-activated K⁺ channels, SK2 is the only one expressed in Purkinje cells. We find reduced pacemaking precision in all Purkinje cells from lobules I-VII and X of SK2^{fl/fl} cerebellar slices. Action potential firing rate is faster and less regular than in WT mice, typically consisting of bursting patterns. This is in agreement with previous studies testing the effects of the SK channel blocker, apamin, on acute cerebellar slices. Apamin application increases Purkinje cell firing frequency, and in most cases, causes tonic firing cells to switch to a bursting mode (Womack and Khodakhah, 2003). The SK2^{fl/fl} Purkinje cell precision deficit extends through the majority of the cerebellum, from lobule X through VII while Purkinje cells in lobules VIII and IX of the SK2^{fl/fl} cerebellum display pacemaking. SK2^{fl/fl} firing behavior in lobules X-VII does not respond to pharmacological manipulation of SK2, whether it be block by apamin or activation by NS309, which increases the calcium affinity of SK2. These results indicate that SK2 makes no measurable contribution to firing patterns in SK2^{fl/fl} Purkinje cells.

Pacemaking deficit in lobules I-VII and X does not cause an overt motor deficit

Previous work has related reduced calcium-activated potassium channel activity with Purkinje cell pacemaking precision, and with motor deficits. Mice lacking large conductance Ca^{2+} -activated potassium channels (BK channels) display overt motor deficits in a variety of assays, including rotarod, balance beam, intention tremor, conditioned eye-blink reflex, and analysis of gait. A high proportion of BK^{-/-} Purkinje cells are silent, and those that fire spend a reduced proportion of time firing tonically. Removing the contribution of BK to the fast AHP lengthens inter-spike intervals. In the absence of the hyperpolarizing effect of BK, depolarization induces inactivation of sodium channels, interrupting the action potential mechanism (Sausbier et al., 2004).

Ca_v and SK channels in precision of Purkinje cell firing

Episodic ataxia type 2 results from mutations in CACNA1 that encodes P/Q-type voltage-gated calcium channels. These mutations reduce current density (Wakamori et al., 1998; Pietrobon, 2002). *In vivo* studies of mice with the spontaneous P/Q-type calcium channel mutation, display disrupted regularity of Purkinje cell simple spikes in the flocculus during optokinetic stimulation. The altered gain and phase of compensatory eye movements in *tottering* are equal to wild-types with flocculus ablation, indicating that this loss of pacemaking precision is tantamount to removing the entire cerebellar circuit from this motor task (Hoebeek et al., 2005). Because mutations in CACNA1 result in human

ataxia, this work suggested that decreased precision of pacemaking might underlie motor deficits.

Because P/Q channels are coupled to SK channels in Purkinje cell dendrites the effects of CACNA1 mutations might be due to reduced SK channel activity (Womack et al., 2004).

Support for this idea was provided by experiments with EBIO, which increases SK2 activation by increasing the apparent calcium sensitivity of SK channels (Strobaek et al., 2004). The motor deficits and dyskinesia of *tottering* mice are partially reversed by *in vivo* EBIO perfusion, indicating that one consequence of reduced P/Q type Ca²⁺ current density is reduced activation of SK channels. Two additional P/Q-type VGCC-related mutants are *ducky* and *leaner*, both of which exhibit deficits in Purkinje cell firing regularity and motor coordination. EBIO restores firing precision in slice recordings from *leaner* and *ducky* mice, and EBIO perfusion ameliorates motor deficits in *ducky* similarly to *tottering* mice (Walter et al., 2006). Recently, *tottering* motor deficits were relieved by oral administration of Chlorzoxazone, a FDA-approved activator of calcium-activated potassium channels (Alvina and Khodakhah, 2010).

The reduced precision of firing and increased overall frequency seen in the SK2^{fl/fl} Purkinje cells suggested that the SK2^{fl/fl} mice might have motor coordination deficits. Despite lacking SK2, there was no overt phenotype during handling. Challenging SK2^{fl/fl} mice with accelerating rotarod and balance beam

assays additionally did not segregate them from WT littermates. Initial comparisons of SK2^{fl/fl} mice and their WT littermates showed no significant difference in their ability to perform and acquire the accelerating rotarod task. SK2^{fl/fl} showed a trend towards superior performance, and a significantly higher performance score during day 2 testing. While the performance score is a less conservative index than repeated measures ANOVA, the result serves to underscore the absence of a deficit in SK2^{fl/fl} mice. Similarly, SK2^{fl/fl} mice and their WT littermates were equally proficient at walking across the balance beam.

Ablation of SK2^{fl/fl} lobules VIII and IX reveals a deficit on balance beam

Our results show that SK2^{fl/fl} mice perform as well as WT mice on the balance beam. Similarly, ablation experiments showed that SK2^{fl/fl}-sham operated mice performed as well as WT-sham operated mice. WT-ablation mice did not display more hindfoot missteps than the WT-sham group, demonstrating that lobules VIII and IX do not comprise the only cerebellar region important for this task. The SK2^{fl/fl}-ablation mice committed increased hindfoot missteps relative to SK2^{fl/fl}-shams, indicating the importance of having at least this small portion of normal pacemaking Purkinje cells. In keeping with this, the SK2^{fl/fl}-ablation group also displayed a greater number of hindfoot missteps than WT-ablation and WT-sham groups. Together, these data demonstrate pacemaking in lobules VIII and IX is

sufficient to perform the balance beam assay. However, VIII and IX are not necessary, as the ablations did not disrupt balance beam performance in WT.

In contrast, the ablation surgeries did not reveal a deficit on the accelerating rotarod, which by extension indicates that the rotarod ability is not dependent on regularity of Purkinje cell firing. This is surprising given that disruption of P/Q-type calcium channels results in robust deficits in rotarod performance, deficits that are ameliorated by EBIO. Poor handling technique during rotarod assays can increase variability of scores to the point that it masks a performance difference between groups. We do not believe that this is the case in this set of experiments because, as noted earlier, SK2^{fl/fl} animals received a higher performance score than WTs in the original comparison. This result was confirmed in two separate cohorts (data not shown) and contradicts the possibility that the variability of scores could hide an SK2^{fl/fl} deficit.

Summary

These results demonstrate that genetic knock-down of SK2 expression in SK2^{fl/fl} mice results in irregular Purkinje cell pacemaking in the majority of lobules within the cerebellar vermis, but that this deficit fails to challenge motor skills required for balance beam and rotarod. A minority of the cerebellar cortex, comprised of lobules VIII and IX, exhibits normal Purkinje cell pacemaking in fl/fl animals. Ablation of this region renders the SK2^{fl/fl} vermis devoid of Purkinje cell

pacemaking, and unmasks a motor deficit assayed by the balance beam. This treatment fails to reveal a deficit on the rotarod, suggesting that Purkinje cell pacemaking in the vermis is not required for this ability.

Chapter IV

Discussion

+V408A and SK2^{fl/fl}, similarities and differences

In this thesis I have described two mouse lines, each based on mutations of a K⁺ channel. Both mice show irregular Purkinje cell firing, and are susceptible to induced motor deficits. There are also differences between these mice. The altered K⁺ channel subunit is expressed presynaptically in basket cell interneurons, increasing GABA release onto postsynaptic Purkinje cells. Conversely, the SK2^{fl/fl} lesion alters intrinsic Purkinje cell pacemaking postsynaptically. The latter is analogous to the EA2 mutations in P/Q-type voltage-gated calcium channels, where motor deficits occur because of insufficient SK2 activation. The lobule-specific dependence on SK2 for regular pacemaking in SK2^{fl/fl} mice suggests that prior work on VGCC mutants (performed in lobule V) might have shown different results if performed in lobules VIII and IX, where the contribution of SK2 is in question.

These mice also differed in their behavioral responses.

The various EA2 mutant mice display motor deficits when challenged with behavioral assays such as the balance beam and accelerating rotarod. Similarly, EA1 mutant mice displayed stress-induced deficits in both assays. However,

unlike EA1 and EA2 mice, SK2^{fl/fl} mice did not show motor deficits in those assays. That is surprising considering that the genetic lesion is “down stream” of the VGCC mutants, and that the majority of lobules in the SK2^{fl/fl} cerebellum display irregular Purkinje cell firing. The lobule specificity of SK2 expression may in part explain the differences between the SK2^{fl/fl} mice and the EA1 mouse or EA2 mouse lines. There is no indication that basket cell expression of Kv1.1 or Purkinje cell expression of P/Q-type Ca²⁺ channels varies across lobules.

Ablation of the remaining SK2^{fl/fl} lobules that display regular pacemaking revealed a motor deficit on balance beam, but not on the accelerating rotarod assay. The differential challenge provided by the balance beam vs. accelerating rotarod is interesting. More interesting is that the SK2^{fl/fl} mice with ablation of VIII and IX retains no vermal Purkinje cells with regular pacemaking, and yet these mice had no deficit on the accelerating rotarod. Further investigation is needed to determine how lesions of the same circuit can diverge in output. This difference could potentially be due to a benefit of reduced SK2 expression in some other circuit that might compensate for deficits in the cerebellum. For example, SK2 block by apamin improves performance in the Morris water maze, and reduces the threshold for LTP induction at the CA3 to CA1 Schaffer collateral synapse in hippocampal slices (Stackman et al., 2002).

How does V408A increase GABA release?

Our findings indicate that increased GABAergic input causes a deficit in pacemaking precision of Purkinje cells. How does the mutation increase GABA release? Electron micrographs provided by our collaborator Rafa Lujan show Kv1.1 subunits expressed in the axons and presynaptic terminals of basket cells, and not in Purkinje cells (Fig. 1). This corroborates previous reports . It may be that reduced K^+ current density of mutant Kv1.1-containing channels in presynaptic terminals results in broadened action potentials and increased probability of release. The higher amplitude of IPSCs in +V408A Purkinje cells indicates an increased success of spontaneous basket cell action potentials to invade the fenestrated presynaptic pinceau structure and elicit release from multiple sites. The frequency of IPSCs is also increased. Our EM data shows Kv1.1 expression in basket cell axons. Reduced Kv1.1 activity in axons could increase the success rate of action potential propagation across axonal branch points, accounting for increased frequency of Purkinje cell IPSCs, with no change in the frequency of spontaneous action potentials in basket cells. Calcium imaging of basket cell action potentials could reveal which sub-cellular compartment has altered function due to this mutation, and tell us more about the role of Kv1.1 in neurotransmitter release.

Subcellular localization of Kv1.1 in the mouse cerebellum

Figure 1. Electron micrographs of the mouse cerebellar cortex showing immunoreactivity for Kv1.1 in basket cell axon and axon terminals, as detected using a pre-embedding immunogold method. (A-B) In the upper part of the granular layer, immunoparticles for Kv1.1 were detected at presynaptic sites along the extrasynaptic membrane (arrows) of the basket cell axonal plexus surrounding the axon initial segment (AIS) of Purkinje cells. (C-E) In the lower part of the molecular layer, immunoparticles for Kv1.1 were detected at presynaptic sites along the extrasynaptic membrane (arrowheads) of basket cell axon terminals (bt) establishing synapses with dendrites (Den) of Purkinje cells (arrows). Immunoparticles for Kv1.1 were also found in axons of basket cells (ax), but not in dendritic spines (ds) of Purkinje cells establishing synapses with parallel fibre (pf). Scale bar: 0.5 μ m. (Rafa Lujan).

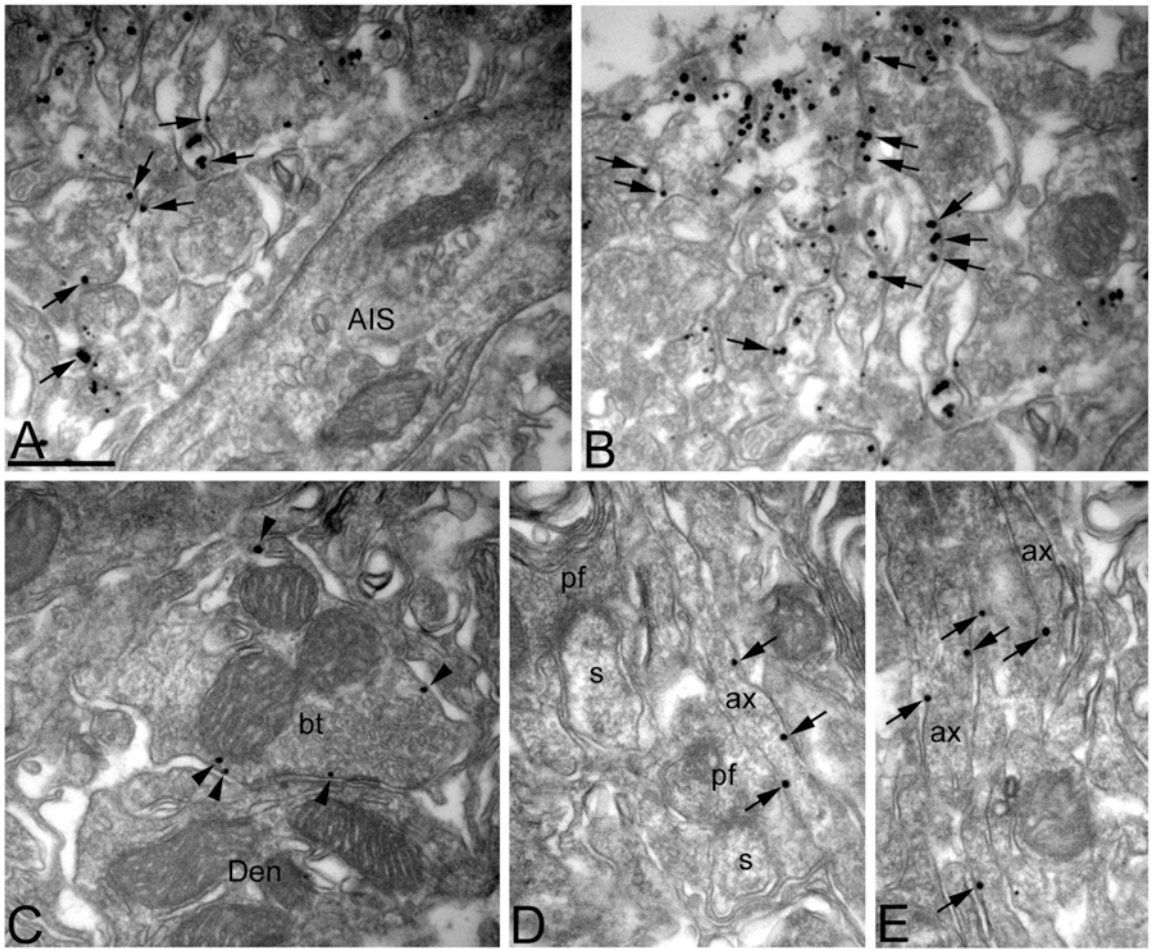


Figure 1.

Kv1.1 heteromeric channel partners

There is evidence that Kv1.1 subunits are predominantly if not always incorporated into heteromeric channels *in vivo* (Coleman et al., 1999). Kv1.1 typically forms heteromeric complexes with other Kv1 family members, particularly 1.2, 1.4, and 1.6. Co-expression of mutant Kv1.1 with WT Kv1.1 demonstrated that the effects of the various loss-of-function mutations are conferred in a dominant negative fashion onto a wide variety of different channels, consisting of all possible stoichiometric combinations with partnering family members and auxiliary subunits.

The identity of partner subunits in part determines the character of the channel, and hence the effect of the mutation. Heteromeric constitution can determine kinetics, pharmacology, and developmental expression changes that are relevant to disease onset. It has not previously been determined what Kv1 subunit forms heteromeric channels with Kv1.1 in basket cell presynaptic terminals. Here we see full colocalization of Kv1.1 and Kv1.2 in the terminal (Fig. 2), indicating the likelihood that these subunits combine to form heteromeric channels.

Figure 2. Kv1.1 colocalizes with Kv1.2 in basket cell terminals. (Rafa Lujan).

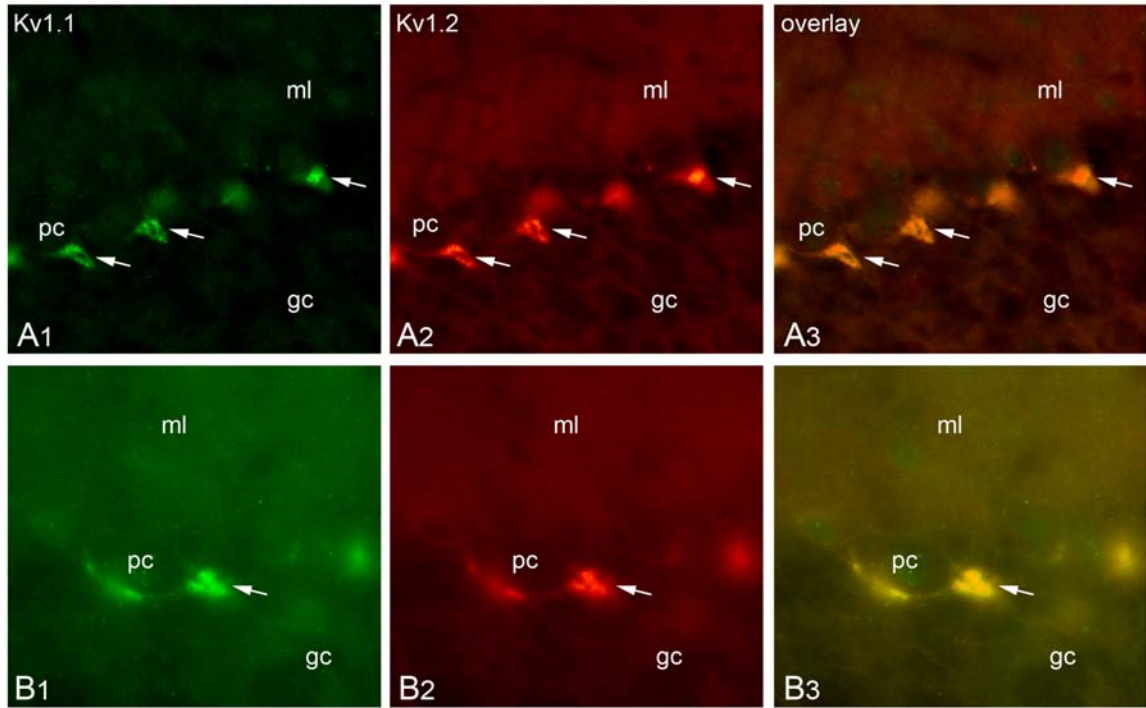


Figure 2.

Lobule-specific SK2 expression

The lobule-specific behavior of SK2^{fl/fl} Purkinje cells was unexpected. SK2^{fl/fl} Purkinje cells from lobule VIII display regular pacemaking, but by what mechanism? Do these Purkinje cells express SK2? Or is SK2 not necessary for regular firing, in this region, even in WT? Preliminary immunolabeling for SK2 across the lobes of WT cerebellum shows strong expression in lobules I-V, but weaker signal in lobules VII-X (most clearly seen in VIII and IX) (**Fig. 3**). Serial sections demonstrated that weaker staining in this region is consistent throughout the vermis, and between immunolabeling experiments. This result suggests that SK2 plays a reduced role in pacemaking in WT Purkinje cells from this region, and that SK2^{fl/fl} Purkinje cells exhibit normal pacemaking in this region because SK2 was never required. This question may be answered by repeating the experiment in SK2^{fl/fl} cerebellar slices (project on-going). Additionally, we have preliminary experiments in SK2^{fl/fl} lobule VIII purkinje cells, testing the sensitivity of pacemaking to apamin. We have not seen convincing sensitivity to apamin (n = 6). We have established lobule specificity of SK2 in the SK2^{fl/fl} cerebellum. Experiments to determine whether this is reflected in WT mice are ongoing.

Figure 3.

Immunolabelling for SK2 in the cerebellum of P60 WT mice, in two sagittal serial sections. (Rafa Lujan).

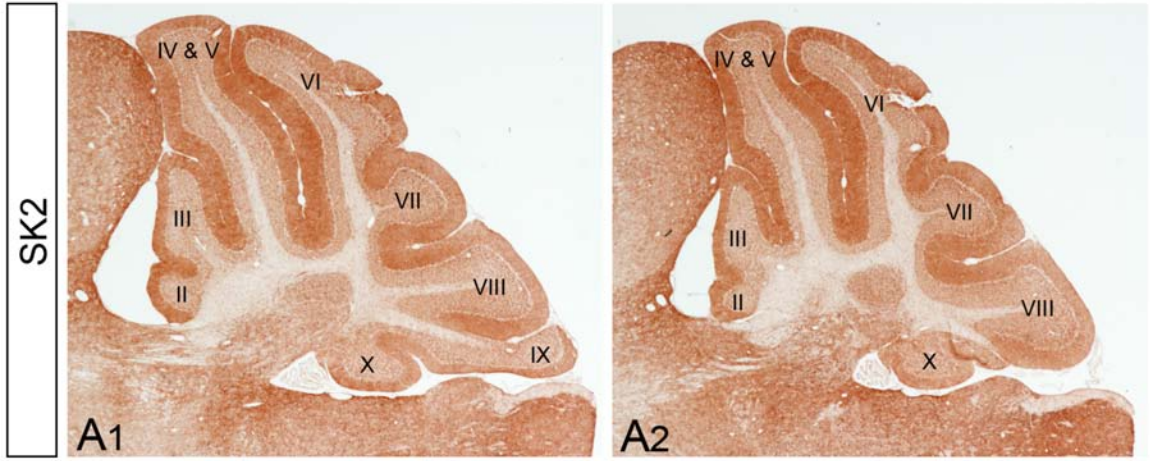


Figure 3.

Summary and conclusions

Experiments in the EA1 mouse model demonstrate that +/V408A Purkinje cells fire action potentials with reduced precision of pacemaking due to increased GABAergic input from interneurons expressing V408A subunit-containing Kv channels. The precision deficit is exacerbated by β AR activation, a model of the effects of stressful events that precipitate attacks in humans. Both the V408A mutation and β AR activation increase GABA release from basket cells, and the effects on Purkinje cell CV_{ISI} are summated. This model is consistent with the need for stress to be coincident with a familial mutation to cause an attack of motor dysfunction. The clinically employed drug, ATZ, ameliorates the +/V408A precision deficit and precludes the majority of the effect of β AR activation on Purkinje cell pacemaking. These results indicate that a reduced precision +/V408A phenotype, exacerbated by β AR activation during stress, underlies motor deficits in EA1. EA1 and EA2 are therefore similar in that ataxia is caused by reduced Purkinje cell pacemaking precision. Unlike any ataxias previously explained, EA1 results from a presynaptic alteration that increases GABAergic inhibition to Purkinje cells.

The experiments with SK2^{fl/fl} mice demonstrate that reduced SK2 expression results in irregular Purkinje cell pacemaking in the majority of lobules within the cerebellar vermis, but that this deficit fails to challenge motor skills required for

balance beam and rotarod. A minority of the cerebellar cortex, comprised of lobules VIII and IX, exhibits normal Purkinje cell pacemaking in SK2^{fl/fl} animals. Ablation of this region renders the SK2^{fl/fl} vermis devoid of Purkinje cell pacemaking, and unmasks a motor deficit assayed by the balance beam. This treatment fails to reveal a deficit on the rotarod, indicating that Purkinje cell pacemaking in the vermis is not required for this ability.

Bibliography

- Adelman JP, Bond CT, Pessia M, Maylie J (1995) Episodic ataxia results from voltage-dependent potassium channels with altered functions. *Neuron* 15:1449-1454.
- Alvina K, Khodakhah K (2010) Calcium-activated potassium channels as therapeutic targets in episodic ataxia type-2. *J Neurosci* 30:7249-7257.
- Ashizawa T, Butler IJ, Harati Y, Roongta SM (1983) A dominantly inherited syndrome with continuous motor neuron discharges. *Ann Neurol* 13:285-290.
- Bell CC, Grimm RJ (1969) Discharge properties of Purkinje cells recorded on single and double microelectrodes. *J Neurophysiol* 32:1044-1055.
- Blatz AL, Magleby KL (1986) Single apamin-blocked Ca^{2+} -activated K^{+} channels of small conductance in cultured rat skeletal muscle. *Nature* 323:718-720.
- Bond C, Sprengel R, Bissonette J, Kaufmann W, Pribnow D, Neelands T, Storck T, Baetscher M, Jerecic J, Maylie J, et al. (2000) Respiration and parturition affected by conditional overexpression of the Ca^{2+} -activated K^{+} channel subunit, SK3. *Science* 289:1942-1946.
- Bond CT, Herson PS, Strassmaier T, Hammond R, Stackman R, Maylie J, Adelman JP (2004) Small conductance Ca^{2+} -activated K^{+} channel knock-

out mice reveal the identity of calcium-dependent afterhyperpolarization currents. *J Neurosci* 280:21231-21236.

Browne DL, Gancher ST, Nutt JG, Brunt ER, Smith EA, Kramer P, Litt M (1994) Episodic ataxia/myokymia syndrome is associated with point mutations in the human potassium channel gene, KCNA1. *Nat Genet* 8:136-140.

Browne DL, Brunt ER, Griggs RC, Nutt JG, Gancher ST, Smith EA, Litt M (1995) Identification of two new KCNA1 mutations in episodic ataxia/myokymia families. *Hum Mol Genet* 4:1671-1672.

Brunt ER, van Weerden TW (1990) Familial paroxysmal kinesigenic ataxia and continuous myokymia. *Brain* 113 (Pt 5):1361-1382.

Cai X, Liang C, Muralidharan S, Kao J, Tang C, Thompson S (2004) Unique roles of SK and Kv4.2 potassium channels in endritic integration. *Neuron* 44:351-364.

Chen X, Kovalchuk Y, Adelsberger H, Henning HA, Sausbier M, Wietzorrek G, Ruth P, Yarom Y, Konnerth A Disruption of the olivo-cerebellar circuit by Purkinje neuron-specific ablation of BK channels. *Proc Natl Acad Sci U S A* 107:12323-12328.

Cingolani LA, Gymnopoulos M, Boccaccio A, Stocker M, Pedarzani P (2002) Developmental regulation of small-conductance Ca²⁺-activated K⁺ channel expression and function in rat Purkinje neurons. *J Neurosci* 11:4456-4467.

- Coetzee WA, Amarillo Y, Chiu J, Chow A, Lau D, McCormack T, Moreno H, Nadal MS, Ozaita A, Pountney D, Saganich M, Vega-Saenz de Miera E, Rudy B (1999) Molecular diversity of K⁺ channels. *Ann NY Acad Sci* 868:233-285.
- Coleman SK, Newcombe J, Pryke J, Dolly JO (1999) Subunit composition of Kv1 channels in human CNS. *J Neurochem* 73:849-858.
- Comu S, Giuliani M, Narayanan V (1996) Episodic ataxia and myokymia syndrome: a new mutation of potassium channel gene Kv1.1. *Ann Neurol* 40:684-687.
- Doyle DA, Morais Cabral J, Pfuetzner RA, Kuo A, Gulbis JM, Cohen SL, Chait BT, MacKinnon R (1998) The structure of the potassium channel: molecular basis of K⁺ conduction and selectivity. *Science* 280:69-77.
- Eccles JC (1973) The cerebellum as a computer: patterns in space and time. *J Physiol*:1-32.
- Edgerton JR, Reinhart PH (2003) Distinct contributions of small and large conductance Ca²⁺-activated K⁺ channels to rat Purkinje neuron function. *J Physiol* 548:53-69.
- Ganchar ST, Nutt JG (1986) Autosomal dominant episodic ataxia: a heterogeneous syndrome. *Mov Disord* 1:239-253.
- Gutman GA, Chandy KG, Fiessmer S, Lazdunski M, McKinnon D, Pardo LA, Robertson GA, Rudy B, Sanguinetti MC, Stuhmer W, all e (2005)

Nomenclature and molecular relationships of voltage-gated potassium channels. *Pharmacol Rev* 57.

Hausser M, Clark BA (1997a) Tonic synaptic inhibition modulates neuronal output pattern and spatiotemporal synaptic integration. *Neuron* 19:665-678.

Hausser M, Clark BA (1997b) Tonic synaptic inhibition modulates neuronal output pattern and spatiotemporal synaptic integration. *Neuron* 19:665-678.

Heginhotham L, Abramson T, MacKinnon R (1992) *Science* 258:1158.

Heginhotham L, Lu Z, Abramson T, MacKinnon R (1994) *J Biophys* 66:1061.

Herson PS, Virk M, Rustay NR, Bond CT, Crabbe JC, Adelman JP, Maylie J (2003) A mouse model of episodic ataxia type-1. *Nat Neurosci* 6:378-383.

Hille B (2001) *Ion Channels of Excitable Membranes*, 3rd Edition. Sunderland, MA.

Hoebeek FE, Stahl JS, van Alpen AM, Schonewille M, Luo C, Rutterman M, van den Maagdenberg AMJM, Molenaar PC, Goossens HHLM, Frens MA, De Zeeuw CI (2005) increased noise level of purkinje cell activities minimizes impact of their modulation during sensorimotor control. *Neuron* 45:953-965.

Hounsgaard J (1979) Pacemaker properties of mammalian Purkinje cells. *Acta Physiol Scand* 106:91-92.

- Ito M (1984) *The Cerebellum and Neural Control*. New York: Raven Press.
- Kandel ER, Schwartz, J.H., and Jessell, T.M. (2000) *Principles of Neural Science* 4th Edition. New York, NY: McGraw-Hill, Health Professions Division.
- Kohler M, Hirshberg B, Bond C, Kinzie J, Marrion N, Maylie J, Adelman J (1996) Small conductance calcium-activated potassium channels from mammalian brain. *Science* 273:1709-1714.
- Kullmann (2002) The neuronal channelopathies. *Brain* 127:1177-1195.
- Lee H, Wang H, Jen JC, Sabatti C, Baloh RW, Nelson SF (2004) A novel mutation in KCNA1 causes episodic ataxia without myokymia. *Hum Mutat* 24:536.
- Li Y, Um SY, McDonald TV (2006) Voltage-gated potassium channels: regulation by accessory subunits. *Neuroscientist* 12:199-210.
- Litt M, Kramer P, Browne D, Gancher S, Brunt ER, Root D, Phromchotikul T, Dubay CJ, Nutt J (1994) A gene for episodic ataxia/myokymia maps to chromosome 12p13. *Am J Hum Genet* 55:702-709.
- Llinas R, Sugimori M (1980) Electrophysiological properties of in vitro Purkinje cell somata in mammalian cerebellar slices. *J Physiol* 305:171-195.
- Long SB, Campbell EB, MacKinnon R (2005) Crystal structure of a mammalian voltage-dependent shaker family K⁺ channel. *Science* 309:897-903.
- Manto M, Pandolfo M (2002) *The cerebellum and its disorders*. Cambridge: Cambridge University Press.

- Manto M, Marmolino D (2009) Cerebellar Ataxias. *Curr Opin Neurol* 22:419-429.
- Maylie B, Bissonnette E, Virk M, Adelman JP, Maylie JG (2002a) Episodic ataxia type 1 mutations in the human Kv1.1 potassium channel alter hKv β 1-induced N-type inactivation. *J Neurosci* 22:4786-4793.
- Maylie B, Bissonnette E, Virk M, Adelman JP, Maylie JG (2002b) Episodic ataxia type 1 mutations in the human Kv1.1 potassium channel alter hKv β 1-induced N-type inactivation. *J Neurosci* 22:4786-4793.
- Miller C (2000) An overview of the potassium channel family. *Genome Biology* 1.
- Mitoma H, Konishi S (1996) Long-lasting facilitation of inhibitory transmission by monoaminergic and cAMP-dependent mechanism in rat cerebellar GABAergic synapses. *Neurosci Lett* 217:141-144.
- Mitoma H, Konishi S (1999) Monoaminergic long-term facilitation of GABA-mediated inhibitory transmission at cerebellar synapses. *Neuroscience* 88:871-883.
- Ngo-Anh TJ, Bloodgood BL, Lin M, Sabatini BL, Maylie J, Adelman JP (2005) SK channels and NMDA receptors form a Ca²⁺-mediated feedback loop in dendritic spines. *Nat Neurosci* 8:642-649.
- Pedarzani P, Mosbacher J, Rivard A, Cingolani L, Oliver D, Stocker M, Adelman J, Fakler B (2001) Control of electrical activity in central neurons by modulating the gating of small conductance Ca²⁺-activated K⁺ channels. *J Biol Chem* 276:9762-9769.

- Pietrobon D (2002) Calcium channels and channelopathies of the central nervous system. *Mol Neurobiol* 25:31-50.
- Raman I, Bean B (1997) Resurgent sodium current and action potential formation in dissociated Purkinje neurons. *J Neurosci* 17:4517-4526.
- Raman IM, Bean BP (1999) Ionic currents underlying spontaneous action potentials in isolated cerebellar Purkinje neurons. *J Neurosci* 19:1663-1674.
- Rustay NR, Wahlsten D, Crabbe JC (2003) Influence of task parameters on rotarod performance and sensitivity to ethanol in mice. *Behav Brain Res* 141:237-249.
- Sailor C, Kaufmann W, Marksteiner J, Knaus H (2004) Comparative immunohistochemical distribution of three small-conductance Ca²⁺-activated potassium channel subunits, SK1, SK2, and SK3 in mouse brain. *Mol Cell Neurosci* 26.
- Saitow F, Konishi S (2000) Excitability increase induced by beta-adrenergic receptor-mediated activation of hyperpolarization-activated cation channels in rat cerebellar basket cells. *J Neurophysiol* 84:2026-2034.
- Saitow F, Satake S, Yamada J, Konishi S (2000) β -adrenergic receptor-mediated presynaptic facilitation of inhibitory GABAergic transmission at cerebellar interneuron-Purkinje cell synapses. *J Neurophysiol* 84:2016-2025.

- Sausbier M, Hu H, Arntz C, etc., Storm JF, Ruth P (2004) Cerebellar ataxia and Purkinje cell dysfunction caused by Ca²⁺-activated K⁺ channel deficiency. PNAS 101:9474-9478.
- Shin S, Hoebeek F, Schonewille M, De Zeeuw C, Aertsen A, De Schutter E (2007) Regular patterns in cerebellar Purkinje cell simple spike trains PLoS One 2:485.
- Southan AP, Robertson B (1998) Patch-clamp recordings from cerebellar basket cell bodies and their presynaptic terminals reveal an asymmetric distribution of voltage-gated potassium channels. J Neurosci 18:948-955.
- Stackman RW, Hammond RS, Linardatos E, Gerlach A, Maylie J, Adelman JP, Tzounopoulos T (2002) Small conductance Ca²⁺-activated K⁺ channels modulate synaptic plasticity and memory encoding. J Neurosci 22:10163-10171.
- Strobaek D, Teuber L, Jorgensen T, Abring P, al. e (2004) Activation of human IK and SK Ca²⁺ activated K⁺ channels by NS309 (6,7-dichloro-1H-indole2,3-dione 3-oxime. Biochim Biophys Acta 1665:1-5.
- Tempel B.L., Papazian D.M., Schwarz T.L., Jan Y.N., L.Y. J (1987) A probable potassium channel component encoded at Shaker locus of drosophila. Science 237:770-775.

- Tsaur ML, Sheng M, Lowenstein DH, Jan YN, Jan LY (1992) Differential expression of K⁺ channel mRNAs in the rat brain and down-regulation in the hippocampus following seizures. *Neuron* 8:1055-1067.
- Wakamori M, Yamazaki K, Matsunodaira H, et al. (1998) Single tottering mutations responsible for the neuropathic phenotype of the P-type calcium channel. *J Biol Chem*:34857-34867.
- Walter JT, Alvina K, Womack MD, Chevez C, Khodakhah K (2006) Decreases in the precision of Purkinje cell pacemaking cause cerebellar dysfunction and ataxia. *Nat Neurosci*.
- Wang H, Kunkel DD, Schwartzkroin PA, Tempel BL (1994) Localization of Kv1.1 and Kv1.2, two K channel proteins, to synaptic terminals, somata, and dendrites in the mouse brain. *J Neurosci* 14:4588-4599.
- Wang H, Kunkel DD, Martin TM, Schwartzkroin PA, Tempel BL (1993) Heteromultimeric K⁺ channels in terminal and juxtaparanodal regions of neurons. *Nature* 365:75-79.
- Womack D, Khodakhah K (2003) Somatic and dendritic small-conductance calcium-activated potassium channels regulate the output of cerebellar Purkinje neurons. *J Neurosci* 23:2600-2607.
- Womack MD, Khodakhah K (2004) Dendritic control of spontaneous bursting in cerebellar Purkinje cells. *J Neurosci* 24:3511-3521.

- Womack MD, Chevez C, Khodakhah K (2004) Calcium-activated potassium channels are selectively coupled to P/Q-type calcium channels in cerebellar Purkinje neurons. *J Neurosci* 24:8818-8822.
- Xia X, Fakler B, Rivard A, Wayman G, Johnson-Pais T, Keen J, Ishii T, Hirschberg B, Bond C, Lutsenko S, Maylie J, Adelman J (1998) Mechanism of calcium gating in small-conductance calcium-activated potassium channels. *Nature* 395:503-507.
- Yu FH, Yarov-Yarovoy V, Gutman GA, Catterall WA (2005) Overview of molecular relationships in the voltage-gated ion channel superfamily. *Pharmacol Rev* 57:387-395.
- Zerr P, Adelman JP, Maylie J (1998a) Episodic ataxia mutations in Kv1.1 alter potassium channel function by dominant negative effects or haploinsufficiency. *J Neurosci* 18:2842-2848.
- Zerr P, Adelman JP, Maylie J (1998b) Characterization of three episodic ataxia mutations in the human Kv1.1 potassium channel. *FEBS Lett* 431:461-464.
- Zuberi SM, Eunson LH, Spauschus A, De Silva R, Tolmie J, Wood NW, McWilliam RC, Stephenson JP, Kullmann DM, Hanna MG (1999) A novel mutation in the human voltage-gated potassium channel gene (Kv1.1) associates with episodic ataxia type 1 and sometimes with partial epilepsy. *Brain* 122 (Pt 5):817-825.